

https://dspace.org/

Phase relation and thermodynamics in Iron-lead-sulphur system.

Ozok, Hakan

1992
https://hdl.handle.net/10539/27916

Downloaded from a DSpace repository. https://dspace.org/

PHASE RELATION AND THERMODYNAMICS IN IRON-LEAD-SULPHUR SYSTEM

BY HAKAN ÖZOK

A dissertation submitted to the Faculty of Engineering, University of the Witwatersrand, Johannesburg, in fulfillment of the requirements for the degree of Master of Science in Engineering.

Johannesburg, 1992

ABSTRACT

PHASE RELATION AND THERMODYNAMICS

IN IRON-LEAD-SULFUR SYSTEM

In this investigation, phase relations and thermodynamic properties in the ternary system Fe-Pb-S were determined.

High temperature phase relations in the FeS-PbS binary system were established by quenching samples equilibrated in evacuated and sealed silica tubes. The eutectic temperature was found to be 842°C at 46 atomic percent PbS. Activities of PbS in this system were measured at 1100° and 1200°C by the dew-point technique, and negative deviations were observed. Krupkowski solution model was applied to the measured activities and experimentaly measured liquidus lines were verified.

Within the Fe-Pb-S ternary system, the boundaries of the immiscibility region together with the tie-line distributions were drawn at 1200°C. Activities of lead were measured by the dew point technique. Furthermore, lead, iron and sulphur activities were calculated by modelling along the ternary miscibility gap.

ACHIEVEMENTS

FeS-PbS phase diagram was redrawn. PbS activities in FeS-PbS melts at 1100, 1200°C were measured and modelled.

Within the Fe-Pb-S ternary system, the boundaries of the ternary miscibility gap were found at 1200°C. Pb activities were measured at 1200°C, Pb, Fe and S activities were calculated by modelling along the miscibility gap.

DECLARATION

I declare that this dissertation is my own, unaided work. It is being submitted for the Master of Science in Engineering at the University of the Witwatersrand, Johannesburg. It has not been submitted before for any degree or examination in any other University.

HAKAN OZOK

25th Day of May 1992

ACKNOWLEDGEMENTS

I would like to express my sincere gratitude to my Supervisor, Professor R H Eric, whose enthusiasm and encouragement has made this project an enriching experience.

Many thanks are extended to the Foundation for Research Development (FRD/CSIR) for financial assistance provided and Council for Mineral Technology (MINTEK) for the chemical analysis performed.

Special thanks to my friend Estelle Toerien for her support and editing of the text.

I am also grateful for the assistance provided by G.Van Der Heever, I. Badenhorst, O. Demir.

TABLE OF CONTENTS

PAGE

Abstract i
Achievements ii
Declaration iii
Acknowledgements iv
Contents v
List of Tables vii
List of figures viii

1. INTRODUCTION 1

2. REVIEW OF LITERATURE 4
   2.1 Phase Relations 4
   2.1.1 The System FeS-PbS 4
   2.1.2 The System Fe-Pb-S 6
   2.2 Thermodynamics 17
   2.2.1 The System FeS-PbS 17
   2.2.2 The System Fe-Pb-S 22

3. EXPERIMENTAL METHODS AND PROCEDURE 26
   3.1 General Remarks on Experimental Procedure 26
   3.2 Starting Materials 26
   3.3 Furnaces and Temperature Control 27
   3.4 Principles of Dew-Point Technique . . . 33
   3.5 Preparation of Dew-Point Probes. 34
   3.6 Measurement of Dew-Point Temperature . . 35
   3.7 Proc re for Quenching Experiments . . . 36
   3.8 Chem l Analyses Procedure 38

4. EXPERIMENTAL RESULTS AND DISCUSSION 40
4.1 Phase Equilibria. 40
4.1.1 Presentation of Results in FeS-PbS system. 40
4.1.2 Discussion of Results in FeS-PbS system. 43
4.1.3 Presentation of Results in Fe-Pb-S system. 45
4.1.4 Discussion of Results in Fe-Pb-S system. 48
4.2. Thermodynamics 49
4.2.1 Presentation of Results in FeS-PbS system. 49
4.2.2 Discussion of Results in FeS-PbS system. 56
4.2.3 Presentation and Discussion of Results in Fe-Pb-S system. 58

5. SUMMARY AND CONCLUSION 78

6. REFERENCE 81

7. APPENDIX 86

LIST OF TABLES

TABLE

		PAGE
1.a	Experimental Data of FeS-PbS Binary System	41
1.b	SEM EDAX Results of FeS-PbS Binary System	42
2.	Experimental Data on Tie-Lines of Fe-Pb-S System at 1200°C	46
3.a	Dew-Point Temperatures in FeS-PbS at 1200°C	53
3.b	Dew-Point Temperatures in FeS-PbS at 1109°C	53
4.	The results of activity calculations	77

LIST OF FIGURES

FIGURE		PAGE
1	FeS-PbS Phase Diagram	5
2	Phase Diagram for the System Pb-PbS	7
3	High temperature portion of the PbS liquids in the system Pb-PbS	8
4	Fe-S phase diagram	11
5	Fe-Pb phase diagram	12
6	Fe-Pb-S liquidus projection	13
7	Fe-Pb-S isothermal section at 859°C	14
8	Fe-Pb-S isothermal section at 730°C	15
9	Activities in FeS-PbS	21
10	Activity data for Fe-S system.	24
11	Activity data for Pb-PbS system	25
12	Vertical section of Dew-point furnace	30
13	Electrical Circuitry of the Dew-point furnace.	31
14	Temperature profile of the Dew-point furnace	32
15	FeS-PbS phase diagram of the present study	44
16	Tie-Lines in Fe-Pb-S system	47
17	FeS-PbS Activity Curves of Present study	55
18	Schematic of an isothermal section in A-B-C system	60
19	Activity coefficient of S versus mole fraction of S	67
20a	Iso-Activities of Fe in the Fe-Pb-S melts at 1200°C	71
20b	Iso-Activities of Pb in the Fe-Pb-S melts at 1200°C	72
20c	Iso-Activities of S in the Fe-Pb-S melts at 1200°C	73
21a	Integration Function for Fe activities	87
21b	Integration Function for Pb activities	88
21c	Integration Function for S activities	89

FIGURE PAGE

22a Integration Function for Fe activities 90
22b Integration Function for S activities 91

1. INTRODUCTION

Current knowledge of the high temperature thermodynamic properties and phase equilibria of many binary and ternary metal-sulphur systems is rather limited and adequate literature is not available. These are essential in the understanding, designing and improvement of the extraction and refining processes, particularly those of non-ferrous metals.

Especially at higher temperatures where liquid phases are involved, this lack of information and data is more pronounced. Solid state regions of metal-sulphur systems received more attention due to the promising electronic and optical properties of some sulphide compounds. Nevertheless, accurate determination of liquidus boundaries and liquid solubility of sulphur in such regions are also essential in order to produce, develop and improve the properties of semiconducting sulphides. On the other hand, for metal extraction processes like smelting, converting or refining, a thorough understanding of thermodynamic activities and thus partial molar quantities of components in liquid solutions as well as phase equilibria are needed.

The above mentioned considerations are particularly true for the Fe-Pb-S ternary system, a knowledge of which is essential for the continuous direct-smelting process of lead sulphide concentrates in high intensity counter-current reactors. The most recent trend in lead production is direct smelting of lead sulphide in a single step. The only known sulphide of lead, galena and sulphides of iron such as pyrite, marcasite and pyrrhotite, occur in nature under a wide range of geological conditions all over the world. Despite prior

processing of lead ore by selective flotation before the smelting operation, certain amounts of iron sulphide still remains in the ore, and during smelting iron sulfide becomes a component of the matte phase. Therefore, an understanding of the equilibrium relations among metal, matte, slag and gas phases is essential for the successful operation and design of the smelting process.

The system involving FeS and PbS is also of interest to researchers belonging to fields other than metallurgy. Geochemists, for example, contributed much of the understanding of phase equilibria in such systems, with the aim of establishing the rock formation behaviour of sulfides, while research by geologists were aimed at correlating and outlining the stability fields of the geologically important assemblages with their occurence in nature.

For a binary or ternary solution phase, many diverse sets of experimental thermodynamic data can be available. Activity of one or more components of various compositions and temperatures can be measured by electromotive force, vapour pressure, mass spectrometric or other techniques. Enthalpies of mixing can be determined calorimetrically. The experimental equilibrium phase diagram is also a source of thermodynamic data. For example, if the standard Gibbs Free Energy of fusion of a stoichiometric component is known, then the activity of this component in the liquid phase can be calculated even nonisothermally along its liquidus. Miscibility gap is also a source of thermodynamic data, since the activity of either component is the same at both ends of the tie-line, even though the actual values of the activities may not be known.

The aim of this work is to generate thermodynamic data on Fe-Pb-S ternary and FeS-PbS pseudo-binary systems by using the Dew-Point and classical equilibration-quenching techniques of thermochemical research. The Dew-Point technique relies upon the high volatility of a component in a metallic or non-metallic solution. The measurements are conducted in a closed system where advantage is taken from the evaporation and condensation phenomena which become a problem in experiments using open systems.

The objective of this study is to obtain specific information with respect to the following:

A. The direction of conjugation lines between the coexisting liquid sulphide and liquid metal phases by quenching experiments at 1200°C and thus determining the boundaries of the immiscibility region (Phase Equilibria Study).

B. Activities of PbS in PbS-FeS melts and activities of Pb in the ternary Fe-Pb-S melts at 1200°C through the Dew-Point measurement (Thermodynamic Study).

C. Calculation and modelling of liquid solutions in the Fe-Pb-S system where results permit.

The information gathered in the steps described above would be applicable to the analysis of the thermodynamics of the Fe-FeS-PbS-Pb portion in the Fe-Pb-S ternary system.

2. REVIEW OF LITERATURE

2.1 PHASE RELATIONS

Many ternary systems of extractive metallurgy which generate interest consist of two metals and one nonmetal such as oxygen or sulphur. In the liquid state, two metals are usually completely soluble in each other, while miscibility gaps often form in the metal-oxygen or metal sulphur binaries, and the immiscibility region extends into the ternary compositions. Usually the composition of one of the liquid phases lies quite close to the pure metal component. For many of the systems, the only information available is that of the tie line distributions in the two liquid fields of the ternary systems.

The information available in literature on systems pertinent to the present study is as follows:

2.1.1 THE SYSTEM FeS-PbS

The FeS-PbS pseudobinary system has been investigated several times (Friedrich[1], Kopylov[2], Kerby[3], Brett[4]). Kerby[3] melted stoichiometric FeS and PbS and found a simple eutectic behaviour, with the eutectic at 835°C and 48 mol % of PbS. Earlier work of Brett[4] and Brett[36] indicated a eutectic temperature of 848°C for the $Fe_{1-x}S$-PbS mixtures. Both phase diagrams are reproduced in Figure 1. The results of Kerby[3] and Brett[4], when considered together, suggest the existence of a eutectic at a composition slightly on the iron sulphide side of the FeS-PbS line, as well as negligible mutual solubilities in solid state.

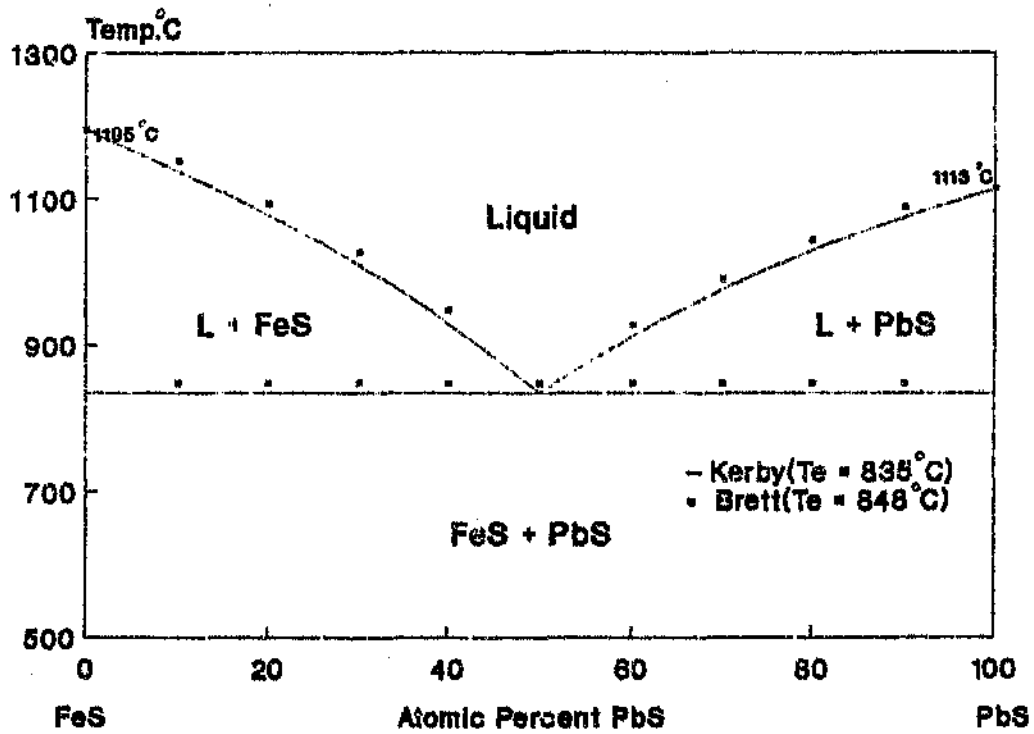


Figure 1. FeS-PbS Phase Diagram. After Kerby[3] and Brett[4]

2.1.2 THE SYSTEM Fe-Pb-S

In the Fe-Pb-S ternary system, the bounding binaries Fe-FeS, Fe-Pb, Pb-PbS are quite well known.

The system Pb-PbS which is of primary interest in lead metallurgy, is a part of the main Pb-S binary. Kullerud[5,6] examined the phase relations in the Pb-S system twice and observed a monotectic and thus liquid immiscibility. His first diagram, represented in Figure 2, showed the monotectic isotherm at 1043°C, and that the monotectic liquid contained 84 mole per cent PbS. In the second diagram, shown by solid lines in Figure 2, the monotectic isotherm did not change much (1041°C), but the composition of monotectic liquid shifted to 65 mole per cent PbS and the immiscibility region was narrower.

Eric[7] has applied the subregular solution model to his experimental data on the Pb-PbS system at 1200°C and constructed a model phase diagram for the high temperature portion of the PbS liquids as shown in Figure 3. Liquidus lines from Miller[8] and Komarek and Hansen[9] were included for comparison. This recent work clearly excluded the possibility of liquid immiscibility at nigh temperatures in the Pb-PbS system.

The thermodynamic and phase equilibrium data of the sub-system Fe-FeS of the Fe-S binary were evaluated by Hillert and Staffanson[8], taking pyrrhotite to be a stoichiometric compound at equal atomic fraction of the components Fe and S. Subsequently, the data for the entire system were evaluated by Sharma and Chang[9] taking into consideration the homogeneity range of pyrrhotite.

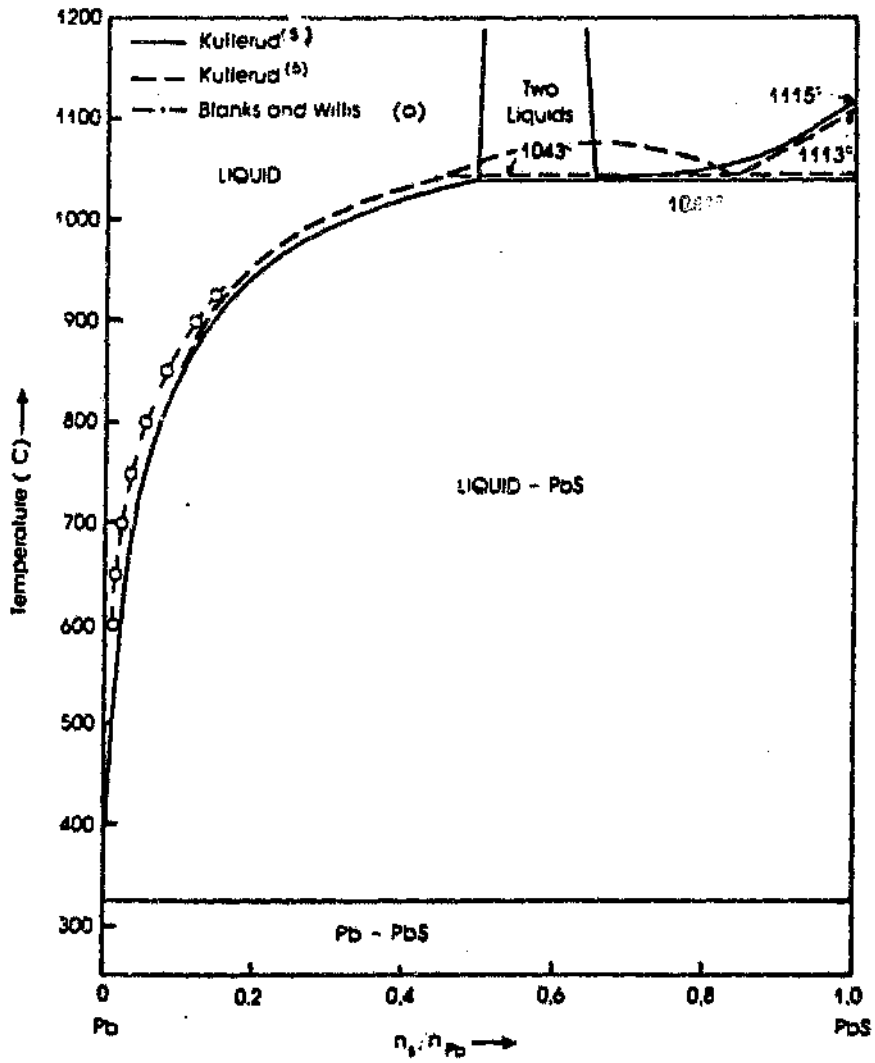


Figure 2. Phase diagram for the system Pb-PbS. After Kullerud[5,6]

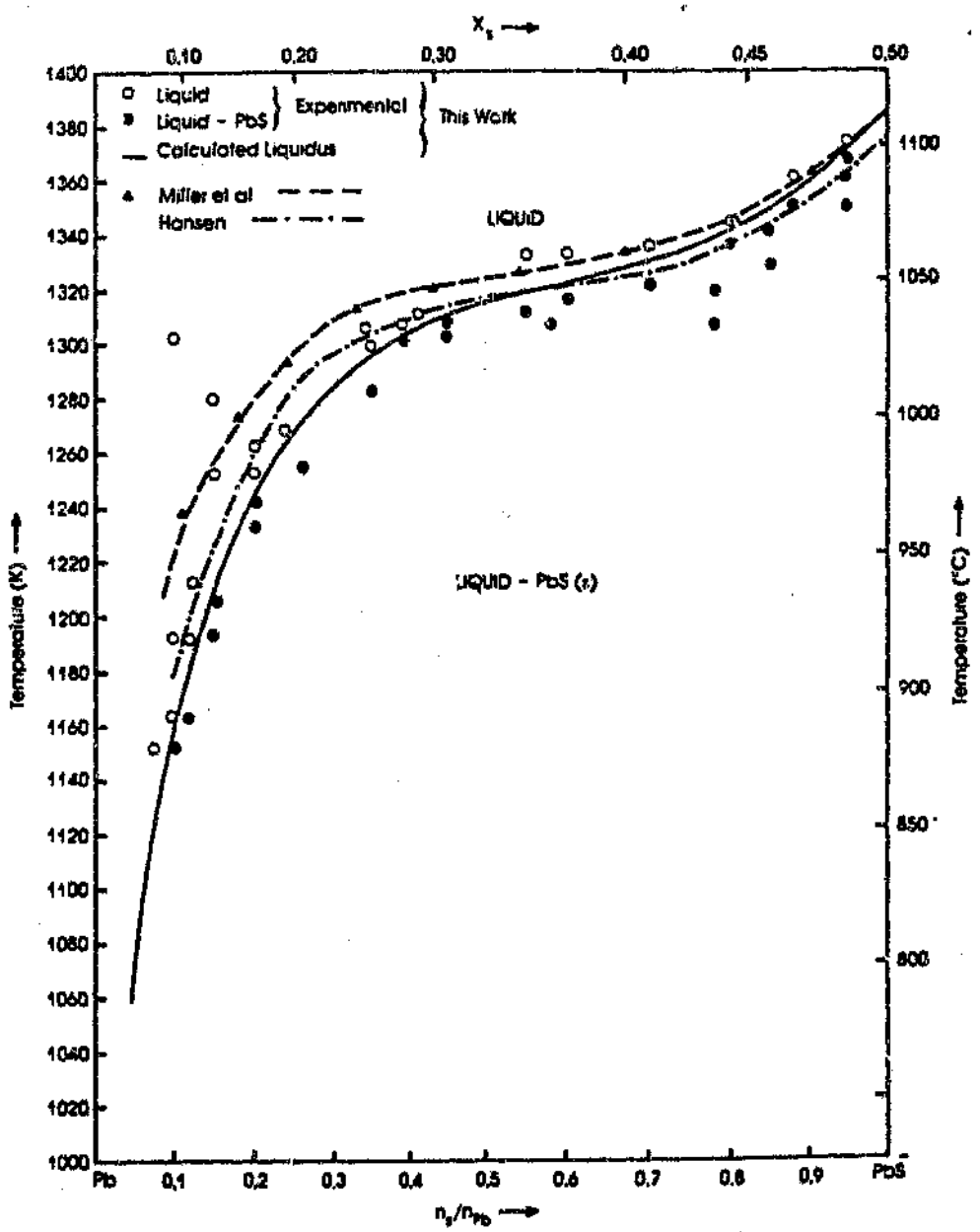


Figure 3. High temperature portion of the PbS liquidus in the system Pb-PbS. After Eriç[7]

For the liquid phase, Sharma and Chang[9] used an associated solution model in order to account for the rapid change of the component activities in the vicinity of equal atomic composition. Recently, Fernandez Guilermant, Hillert, Jonson, and Sundman[10] re-evaluated the Fe-S system using a two sub-lattice model for the liquid and pyrrhotite phases. Chuang, Hsieh, Austin Chang[11] also re-evaluated the Fe-S system, as shown in Figure 4, using the same models as Sharma and Chang[9] for the liquid and pyrrhotite phase. This is an improvement of the earlier evaluation of Sharma and Chang.

Due to the extremely small mutual solubilities of iron and lead, the Fe-Pb phase diagram has not been determined fully. Kubachewski[12] estimated the solubility of lead in liquid iron between 1530 and 1700°C as :

$$\log (\text{at.\%Pb}) = -13,400/T(K) + 6.16 \qquad (1)$$

The solubility of iron in liquid lead varies from 8.10^{-4} at.% Fe at 600°C to about 0.2 at.% Fe at 1300°C. A monotectic reaction occurs at 1530°C, where liquid of 0.05 at.% Pb yields bcc iron(α) with 2.7×10^{-4} at.% Pb and a lead-rich liquid.

The invariant reactions corresponding to the polymorphic transformations in iron and final solidification of lead are not known. Fe-Pb binary phase diagram is shown in Figure 5.

The information available on Fe-Pb-S ternary system comes mainly from the work of Brett[4], who studied the FeS-S-PbS region. On the basis of their experiments on compositions that lie in the FeS-S-PbS

region of the ternary diagram, a liquidus surface was drawn, as given in Figure 6. The primary regions of crystallization are; $Fe_{1-x}S$, FeS_2, PbS and S. A ternary monotectic reaction M_2 occurs at 716°C. At 723°C, the ternary liquid composition crosses the FeS_2-PbS line and at 848°C, it crosses the Fe_{1-x}-PbS line. The peritectic univariant line that starts at 743°C from p_2 on the Fe-S side meets the monotectic line m_2 from the Fe-S side at 740°C to undergo the U_4 reaction (Figure 6).

The two liquidus lines resulting from this transition reaction go from U_4' to meet the U_5 and the M_2 points at 719 and 716°C respectively.

$S_{(l)}$ is a product of the monotectic reaction M_2. Its solidification occurs through a ternary eutectic reaction E_2 postulated at about 114°C, close to the sulphur corner.

Not much is known about the liquidus surface for the bottom half of the triangle, that is, in the Fe-FeS-PbS-Pb region. Brett[4] indicated the possibility of the occurence of another ternary liquid in this region. Assuming this to be the case a hypothetical surface for this region was included in Figure 6. The regions of primary crystallizations are α, γ , $Fe_{1-x}S$, PbS and Pb. Two transitions U_1 and U_2 occur before (i.e. at higher temperature) the ternary liquid reaches a ternary monotectic reaction plane (M_1), assumed to be at about 800°C.

Brett[4] gave five isothermal sections at 730, 720, 716, 730 and 850°C in their earlier work[13]. Figure 7 and 8 give the isothermal sections at 850 and 730°C after slight modifications to match the binary data.

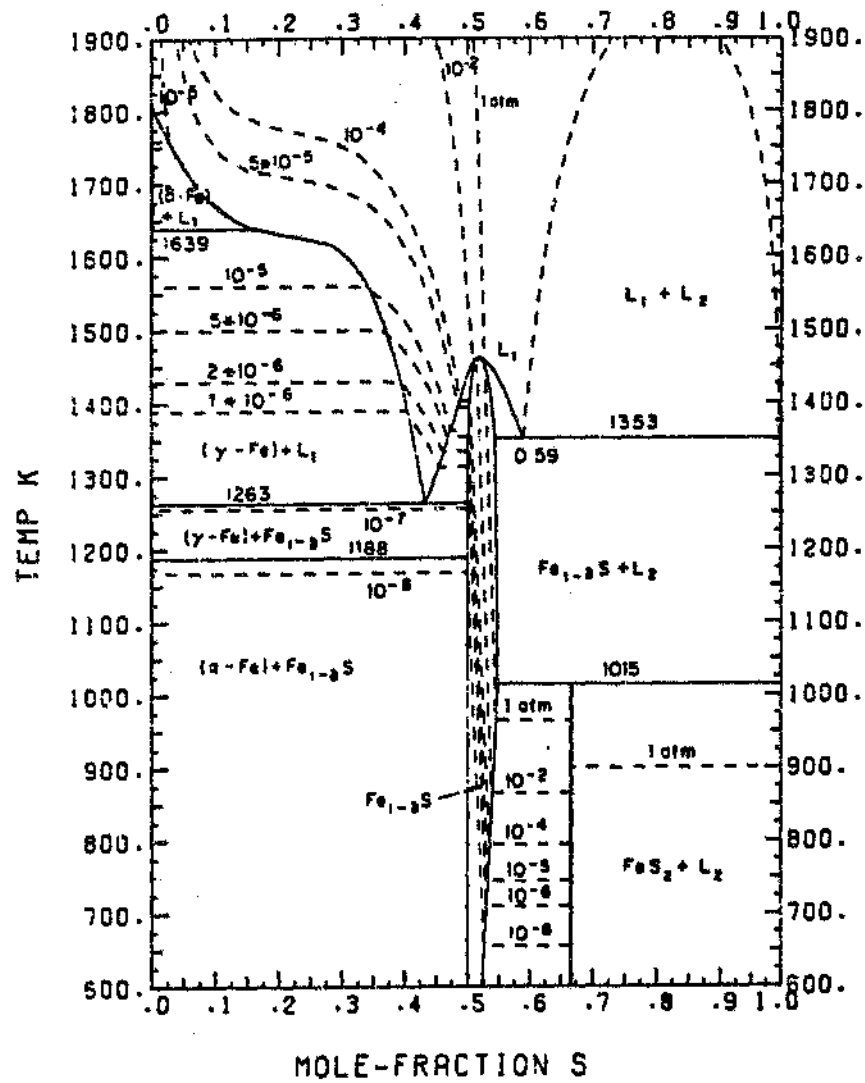


Figure 4. Fe-S phase diagram with isobar values of $S_2(g)$ up to latm=1.01325x10^{+5} pa. The critical temperature of pure S is 1313K. After YY Chuang, KC Hsieh and YA Chang[11]

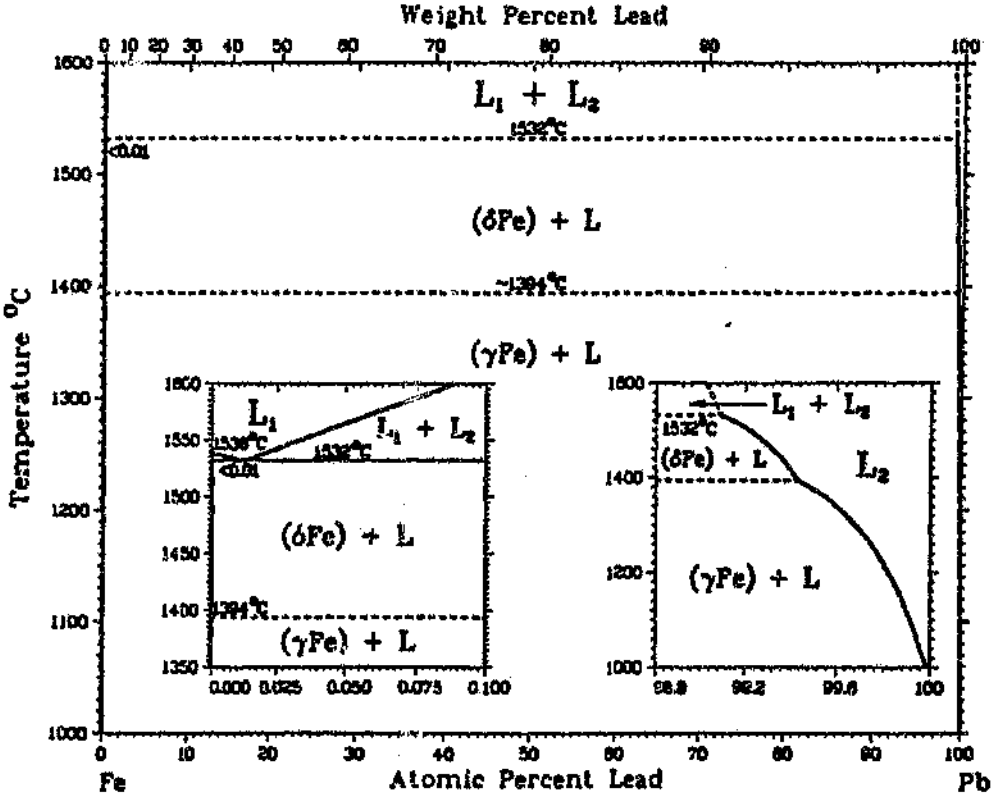


Figure 5. Fe-Pb phase diagram.

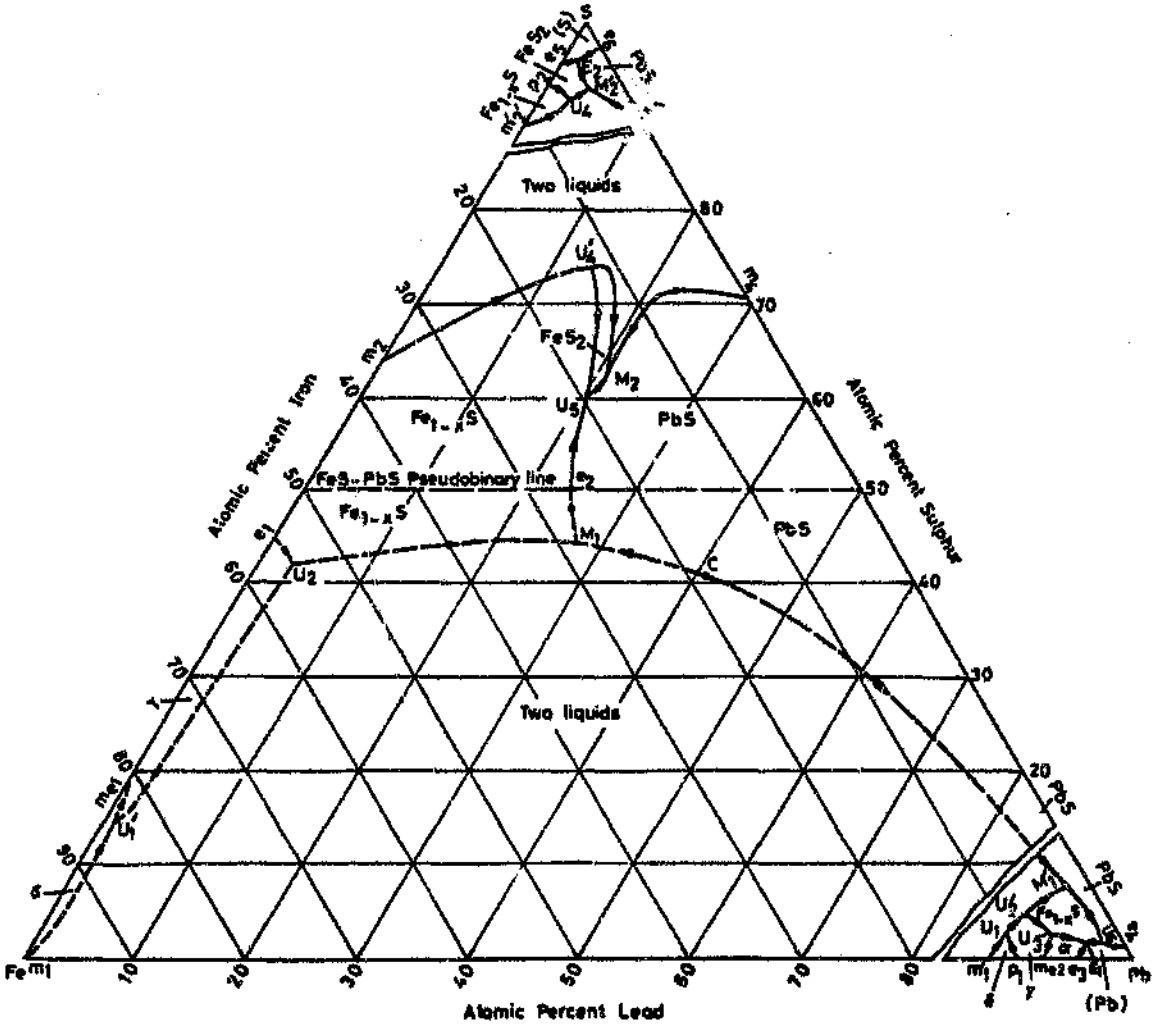


Figure 6. Fe-Pb-S liquidus projection in atomic percent. After Brett[4].

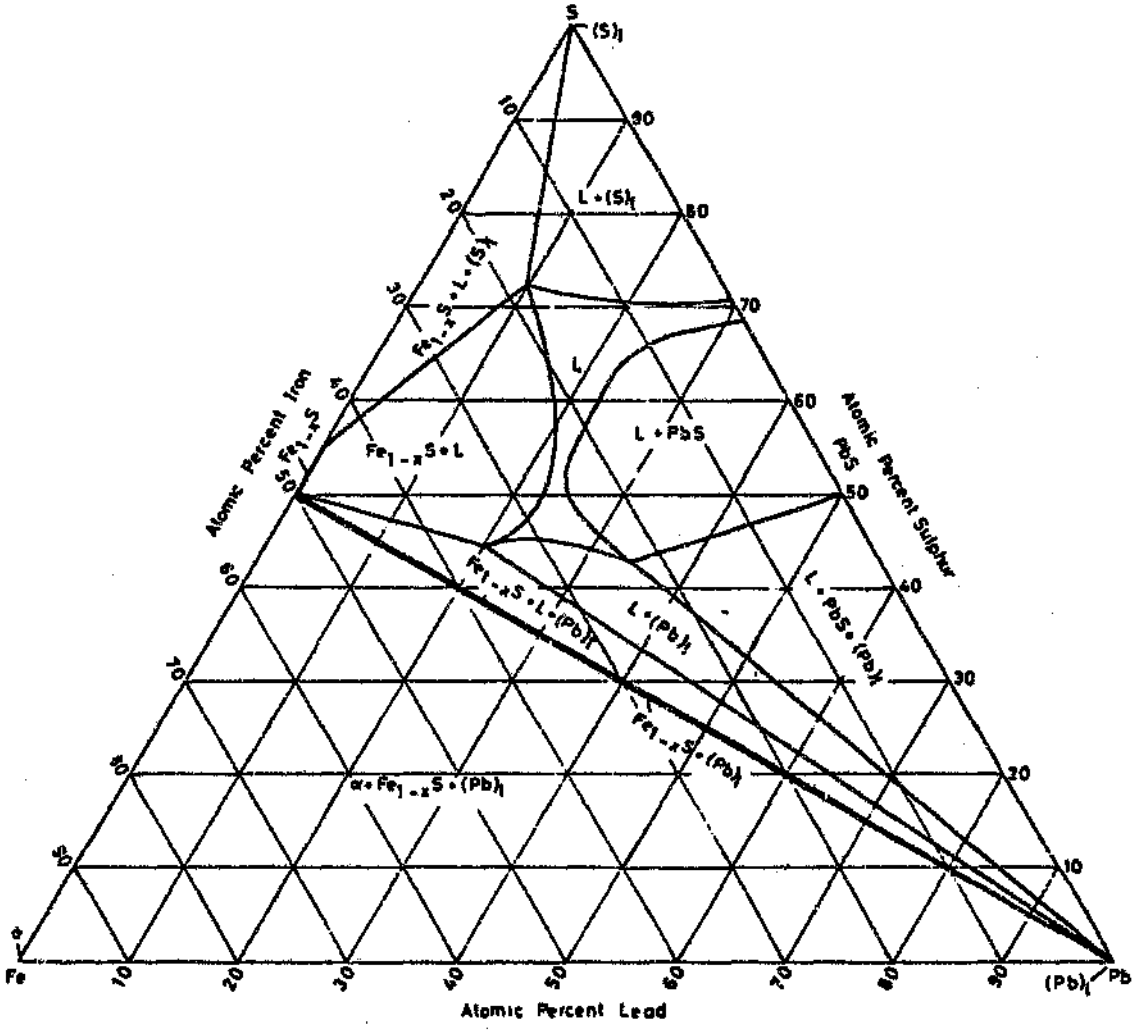


Figure 7. Fe-Pb-S isothermal section at 850°C in atomic percent. After Brett[4].

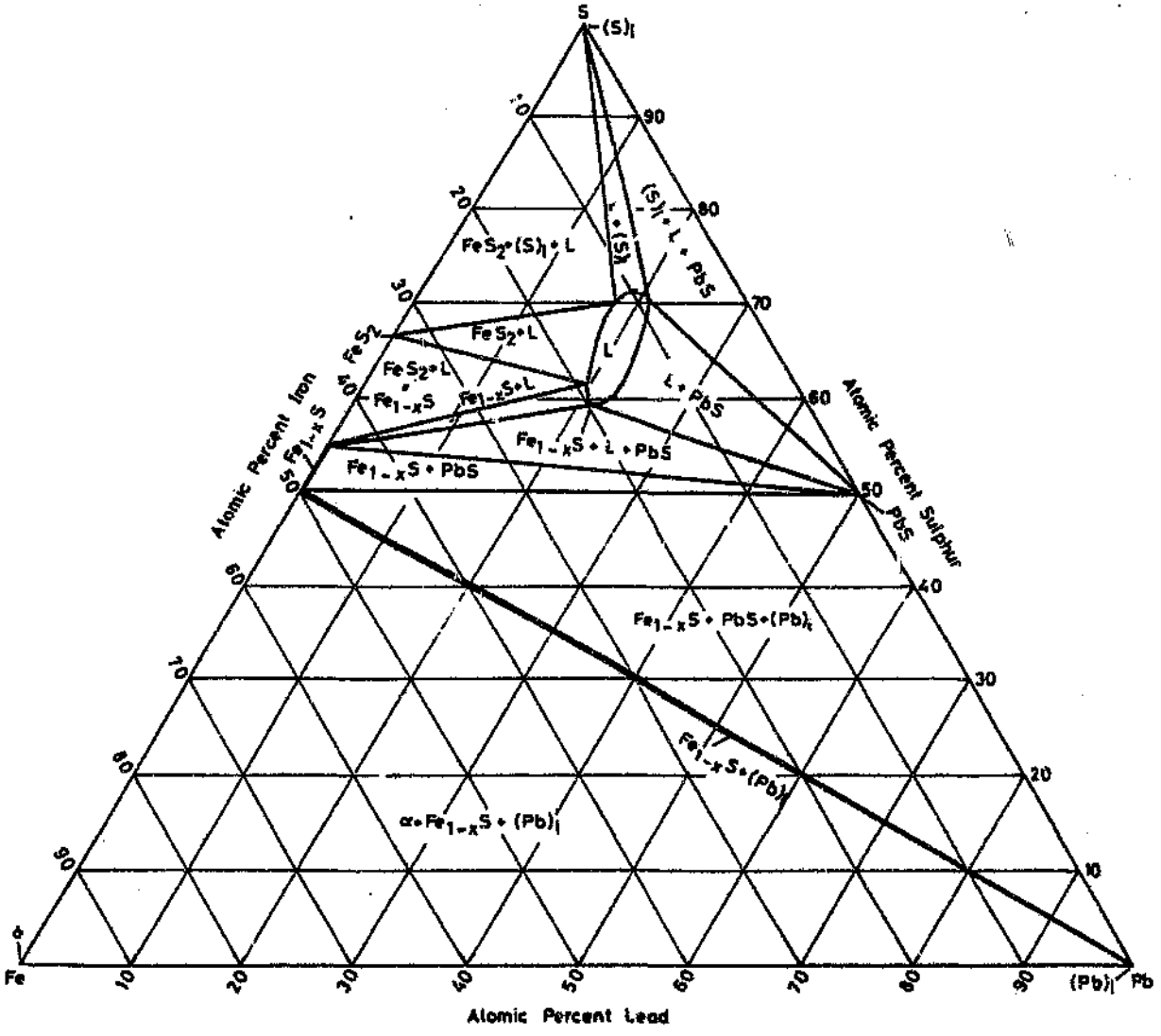


Figure 8. Fe-Pb-S isothermal section at 730°C in atomic percent. After Brett[4].

2.2 THERMODYNAMICS

The available information relevant to the present study is summarized in the following subsections.

2.2.1 THE SYSTEM FeS-PbS

Lead sulphide is highly volatile and this high volatility is maintained over a broad range of sulphur pressures. This behaviour represents a challenge to the engineer searching for an effective means of separating lead from raw materials.

Eriç and Timuçin[18] have used the following vapor pressure equations for pure PbS:

$$\log P_{PbS}(atm) = -11\ 694/T + 7.497 \qquad (2)$$

$$\log P_{PbS}(atm) = -9114/T + 5.636 \qquad (3)$$

Equation 2 and 3 are reported[18] to be valid in the temperature ranges T<1113° and T>1113°C respectively.

Equation 2 was derived[14] from the vaporization data of Colin and Drowart[23]. Numerous linear equations, similar to equation 3, are available[14,37,38] to express the vapor pressures of pure liquid PbS; the constants of various equations, and hence the values of P_{PbS}, are affected by the heat of fusion value, ΔH_f, selected for PbS. Equation 3 is obtained[18] by combining Equation 2 with the value 49 400 J/mole measured by Shamsuddin[16] for ΔH_f of PbS. Schuhmann[14] assigned a value of 46 423 J/mole to ΔH_f so that the resulting vapor pressure equation could be used to describe the behaviour of

Pb-PbS solutions. The P_{PbS} values calculated from their equation were within 2 pct of those given by Equation 3.

Colin and Drowart[23] studied the vaporization chemistry of PbS by mass spectrometric measurements and determined the composition of the lead sulphide vapor phase as a function of temperature in the interval 979 to 1182 K. Their results reveal that the vapor phase consists of species PbS, Pb_2S_2, Pb and S_2 where PbS is by far the predominant component. From an extrapolation of the data[23] to 1200°C, it can be estimated that the concentration of Pb and Pb_2S_2 will be less than 1 pct each and that of S_2 will be negligibly small in the gas phase.

The change in standard free energy attending the fusion of PbS according to the reaction:

$$PbS(s) = PbS(l) \qquad (4)$$

has been estimated[14] as

$$\Delta G^\circ = 46423-33.45T \text{ J/mole} \qquad (5)$$

The enthalpy of fusion (46423 J/mole) in this equation was made higher than the value recommended by Elliott and Gleiser[15] (36418 J/mole) in order to keep the regular solution model for Pb-PbS solutions valid over the entire composition range as was already discussed above. This arbitrary value compares fairly well with the direct measurement of Shamsuddin[16], who reported a value of 49400 ± 2100 J/mole for the enthalpy of fusion of PbS obtained by DTA calorimetry. The standard free

energy of fusion calculated by using this new enthalpy is

$$\Delta G^{\circ} = 49400 - 35{,}64\ T\ J/mole \qquad (6)$$

This equation was used in the calculations necessary for this study.

In equation (6) the melting point of PbS was taken as 1113°C, and variation of PbS activity with temperature can be expressed as:

$$\ln a_{PbS} = -5942/T + 4.287 \qquad (7)$$

There are several expressions on the standard free energy of formation of pure solid and liquid PbS. For the equilibrium:

$$Pb(l) + \tfrac{1}{2}S_2(g) = PbS(s) \qquad (8)$$

Schuhmann[14] modified the change in standard free energy as:

$$\Delta G^{\circ} = -159905 + 84.35T\ J/mole \qquad (9)$$

By adding equilibrium (8) to equilibrium (4) and equation (6) to equation (9), the standard free energy of formation of liquid PbS can be obtained as:

$$Pb(l) + \tfrac{1}{2}S_2(g) = PbS(l) \qquad (10)$$

and

$$\Delta G^{\circ} = -110505 + 48.71T\ J/mole \qquad (11)$$

Throughout this investigation equation (11) was

employed to calculate the standard free energy of formation of liquid PbS.

The following vapor-pressure equation for Pb within the temperature interval of 1100 K $\leq T \leq$ 1500 K was derived from the vaporization data for lead compiled by Kellog[35].

$$\log a_{Pb}(atm) = -9558/T + 4.7475 \qquad (12)$$

The Gibbs free energy difference for the reaction

$$\tfrac{1}{2}S_2 g = S(l) \qquad (13)$$

was calculated at 1473 K as ΔG°=33065.77 J/mole from JANAF data[41].

The change in the standard free energy of formation of liquid FeS for the reaction

$$Fe(l) + \tfrac{1}{2}S_2(g) = FeS(l) \qquad (14)$$

was reported by Hillert and Staffanssons[36] as

$$\Delta G^\circ = -148\ 841.6 + 50.8\ T\ (J/mole) \qquad (15)$$

For melting of FeS[17]

$$FeS(s) = FeS(l) \qquad (16)$$

$$\Delta G^\circ = 32310.7 + 22.01\ T\ (J/mole) \qquad (17)$$

from which the following activity equation for FeS can be obtained:

$$\ln a_{FeS} = -3886.1/T + 2.647 \qquad (18)$$

Eriç[18] calculated activities of PbS in FeS - PbS liquid solutions at 1200°C by using their experimental data, and found an ideal behaviour. However, a previous study, Nesterov[19] observed a negative departures from ideality on their measurements of PbS activities of XPbS ≤ 0.35 in the range of 1000 - 1250°C. The PbS activities determined by both of the investigators are substantially different as shown in Figure 9. Nesterov et al[19] have derived a vapor pressure equation for PbS from transport measurements in the range 850° to 1100°C and extrapolated this up to 1250°C without considering the change of state in PbS and estimated a negative behaviour. On the other hand, the ideal behaviour obtained by Eriç[18] would be affected by the higher measured dew point temperatures of PbS. In fact, the author reported[18] the need to again investigate the phase relations in this system because of the anomaly observed in PbS activities obtained from the PbS branch of liquidus.

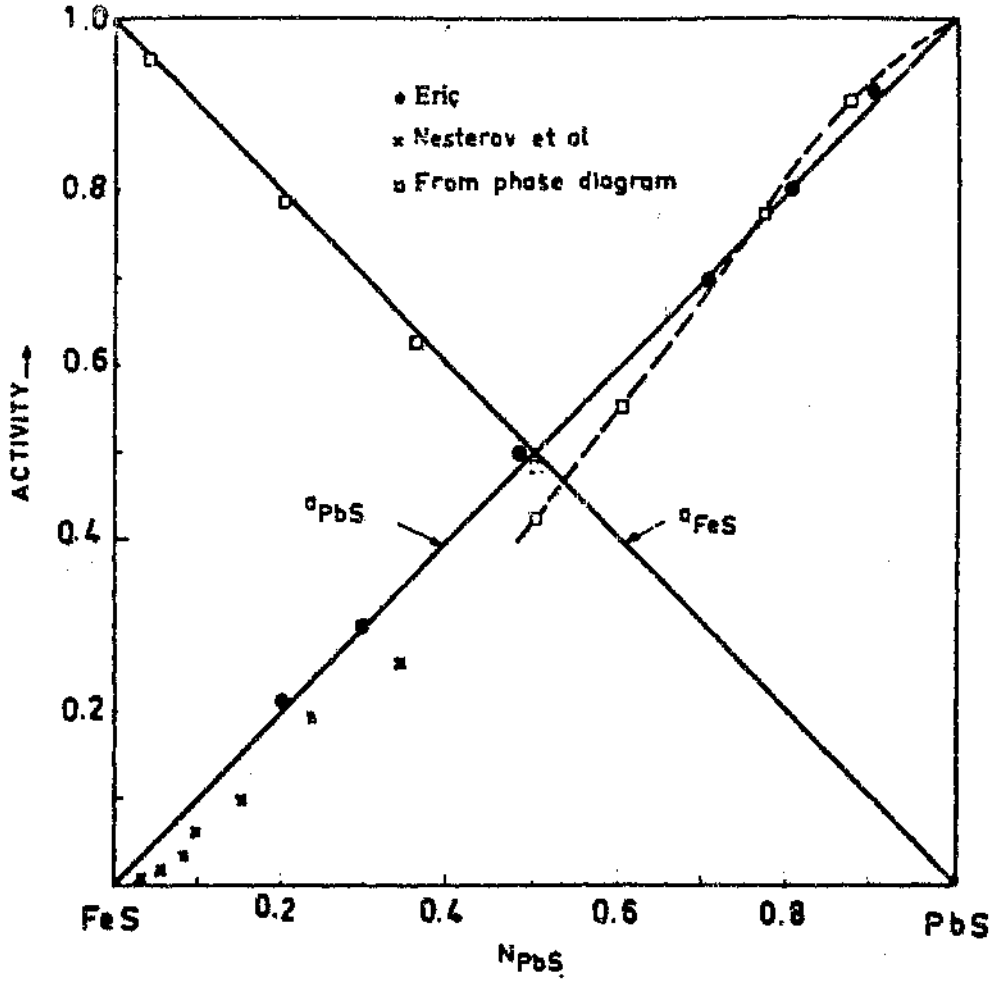


Figure 9. Activity composition relations in FeS-PbS melts at 1200°C. After Eriç[18] and Nesterov et al[19].

2.2.1 THE SYSTEM Fe-Pb-S

There are no experimentally measured or indirectly calculated activities of components within the ternary field or miscibility gap of the Fe-Pb-S system. In the Fe-Pb-S system, thermodynamic properties in the bounding binaries Fe-FeS and Pb-PbS are quite well known.

The Fe-S binary is characterized by a congruent melting phase, pyrrhotite, at about 50 atomic percent S, and eutectic between Fe and pyrrhotite and a monotectic between pyrrhotite and S[11,20]. The liquidus in equilibrium with Fe at about 20 atomic percent S is rather flat, suggesting a tendency toward immiscibility in the liquid. Pyrrhotite has ordered NiAs structure ($B8_1$) and exists over a rather large range of homogeneity. The general features of the phase relationships in the Fe-S binary suggests a stable liquid solution around 50 atomic percent S and relatively weak solutions on either side of the equa-atomic composition. The activity data of sulfur in the liquid phase increases monotonously from pure Fe to about 50 atomic percent S and then increases rapidly with composition, similar to that of component in a highly stable solid phase[11,21,22].

Chuang[11] estimated sulfur activities from pure iron to $X_S = 0.5$. Their calculations and the results obtained by other researchers are shown in Figure 10.

In literature thermodynamic activities of components of Pb-PbS system are available from the experimental

study of Eriç and Timuçin[7]. They have measured PbS activities in the Pb-PbS system by using isopiestic technique at 1200°C. This technique involved the equilibration of Pb-PbS samples with Cu_2S-PbS samples of known activity through the vapor phase in sealed silica capsules. Activity composition diagram[7] in Pb-PbS melts at 1473 K is shown in Figure 11. Activities of both components show positive departures from the ideal in accord with the experimentally determined phase diagram. Eriç[7] has calculated the activities of PbS and Pb by employing the subregular solution model and also derived an analytical expression describing the position of the PbS liquidus. The model liquidus and activities were in excellent agreement with the actual direct experimental results. The activities reported by Yazawa et al[37] are considerably higher than the values estimated by Eriç[7]. Yazawa[37] measured PbS vapor pressure over Pb-PbS solutions by the transpiration-carrier gas method. In such systems, both Pb and PbS are vaporized from Pb-PbS melts, and they apparently measured the sum of P_{Pb} and P_{PbS}, rather than only P_{PbS}, which would explain the high activities derived.

There is no measured activity data for the system Fe-Pb in literature, but since the components are virtually immiscible in each other, their activities will always be around 1.0.

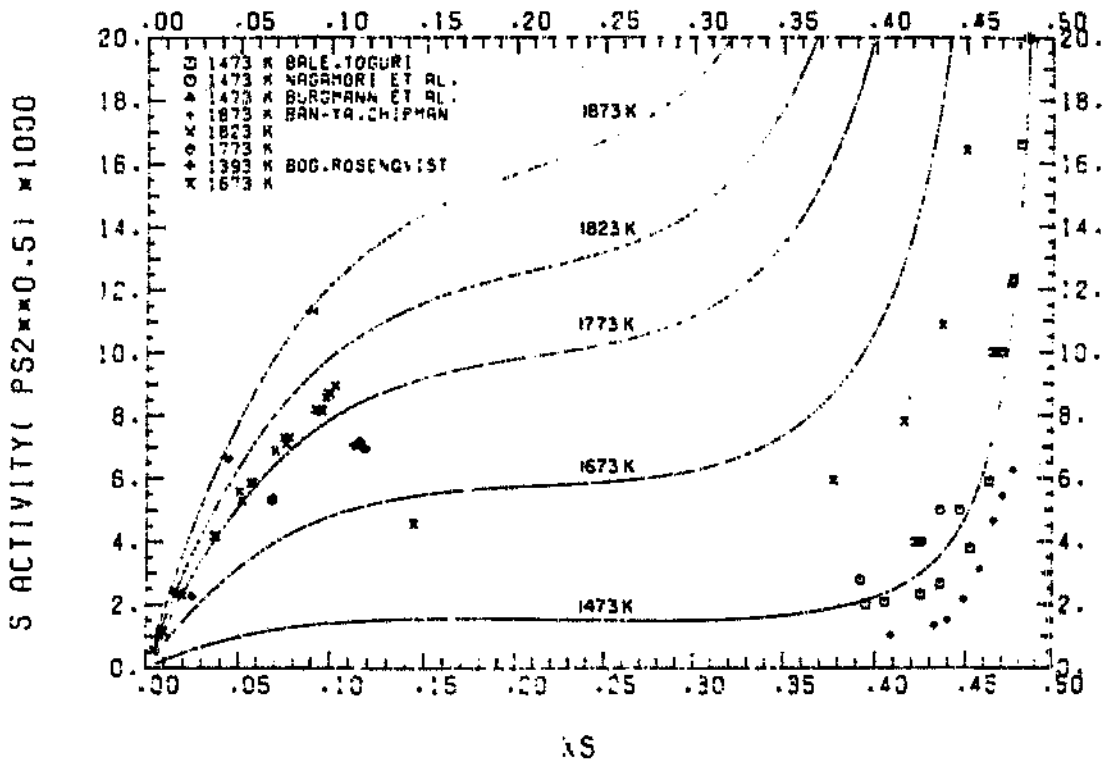


Figure 10. Activity data for Fe-S system at 1473 to 1873K. After Chuang[11].

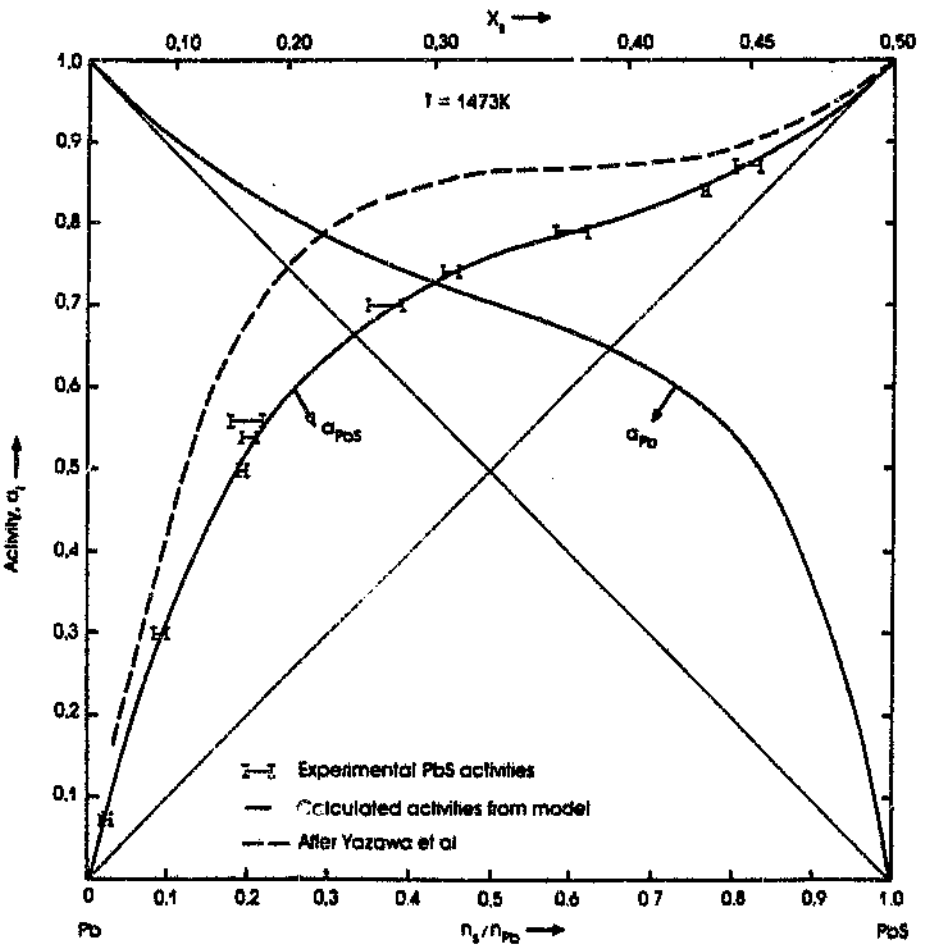


Figure 11. Activity composition diagram in Pb-PbS melts at 1473 K. After Friç.

3. EXPERIMENTAL METHODS AND PROCEDURE

3.1 GENERAL REMARKS ON EXPERIMENTAL PROCEDURE

Phase equilibrium studies in the systems FeS-PbS and Fe-Pb-S were performed by using the quenching method. For this purpose, samples belonging to these systems were placed in evacuated silica capsules and heated in a vertical tube furnace at selected temperatures until equilibrium phases had developed. The capsules were subsequently quenched into water, and the phases were examined metallographically. Portions of quenched samples were analyzed chemically and by Energy Dispersive Analyses of X-Ray (EDAX) in order to ascertain the compositions of phases. The data obtained were used to delineate the liquidus lines in the FeS-PbS system, and the distribution of conjugation lines between co-existing liquids in the Fe-Pb-S system.

For activity measurements, the dew-point method was used. Other methods, like gas equilibration and emf measurements which operates well in open systems were inapplicable in the present study owing to the condensation of PbS vapors in cooler parts of the furnace tube.

In the course of activity measurements, activities of PbS in FeS-PbS binary systems were determined by the dew-point method at 1100 and 1200°C, as well as those of Pb along the ternary miscibility gap of the Fe-Pb-S system.

3.2 STARTING MATERIALS

The primary starting materials were pure Fe, Pb, S. The

source of iron was fine electrolytic powder of 99.9 % purity from South African Chemicals. Sulphur, from the same source, also had 99.9% purity. Analytical reagent grade granular lead was melted and solidified in small alumina crucibles under a flow of hydrogen gas at 500°C in a horizontal tube furnace prior to use.

Lead sulphide was prepared by reacting a stoichiometric mixture of lead and sulphur step wise at temperatures 600°C to 1200°C. Lead chips and sulphur pellets, forming a total mass of about 30 grams, were placed in a silica tube. The tube was evacuated to approximately 5×10^{-5} torr with the help of a rotary-diffusion pump unit, sealed by hydrogen torch and then heated at 600°C for a week. Thereafter the temperature was increased up to 1200°C by 200°C increments per day. The heating at 1200°C was for 2 hours. Lead and sulphur became molten in the first stage low temperature processing, forming solid PbS. At the last stage heating, PbS was melted for homogenizing the entire product. The PbS so formed and homogenized was cooled to room temperature, removed from the silica tube, and analyzed by X ray diffraction to verify that the final product was completely PbS.

Iron sulphide was synthesized from its elements by the same procedure described for the production of PbS.

3.3 FURNACES AND TEMPERATURE CONTROL

Three different furnaces were employed in this investigation. Muffle furnace heated by silicon carbide elements was used during the syntheses of starting sulphides. This furnace could operate at temperatures in excess of 1200°C; temperatures inside the muffle were

maintained within ±10°C of their set values by an Eurotherm on/off controller activated through a Platinum/Platinum-13% Rhodium thermocouple.

The second furnace was a vertical alumina tube furnace which could reach 1250°C by a wound kanthal wire heating element. This arrangement provided a 5 cm. long uniform hot zone over which the temperatures could be maintained constant within ±1°C by means of thyristor coupled Eurotherm controller activated through a Platinum / Platinum-13% Rhodium thermocouple. This vertical type tube furnace was used for the phase equilibrium studies in the FeS-PbS and Fe-Pb-S systems.

The last of the heating units which proved to be the major tool of experimentation for activity determinations was the Dew-Point furnace (DPF). Since such furnaces have to be built according to specific needs for research, they are not manufactured commercially.

A vertical section through the midplane of the DPF used in this study is shown in Figure 12. The main mullite furnace tube, 46 cm long, 26 mm in diameter carried four different heating coils wound from 0.71 mm kanthal wire. The first three coils at the bottom were connected by the electrical circuit shown in Figure 13. The resistors in series with the second and third coils were adjustable so that the input power could be distributed between the three coils to obtain any desired temperature profile along the furnace tube. A typical temperature-distance curve is shown in Figure 14. The control of temperature along these bottom coils was accomplished by a Eurotherm temperature controller coupled to a tyristor unit. The fourth and topmost coil was powered and controlled seperately from the others with the aid of its own

Eurotherm temperature controller. Both temperature controllers were activated by Pt/Pt-13% Rh thermocouples. This arrangement permitted the manipulation of temperatures at the tip of the silica sample tube to within ±½°C of the set temperature values.

A 33 cm long and 16 mm in diameter quartz tube was inserted into the DPF tube to help minimize the temperature gradients. Between the third and fourth coils two 7 mm diameter alumina tubes were inserted in transverse positions into the furnace tube for the purpose of viewing the tip of the sample tube. Each of these alumina tubes were 10 cm in length.

An alumina plug with a vertical alumina tube for sample tube positioning was used to cover the top of the DPF tube. A Pt/Pt-13% Rh thermocouple was suspended through the alumina tube of the plug to measure the temperature at the tip of the sample tube. The temperature at the bottom of the liquid sample was measured by means of a second Pt/Pt-13% Rh thermocouple led through the hole of the cemented alumina pedestal which was supported by a 13 mm diameter quartz tube.

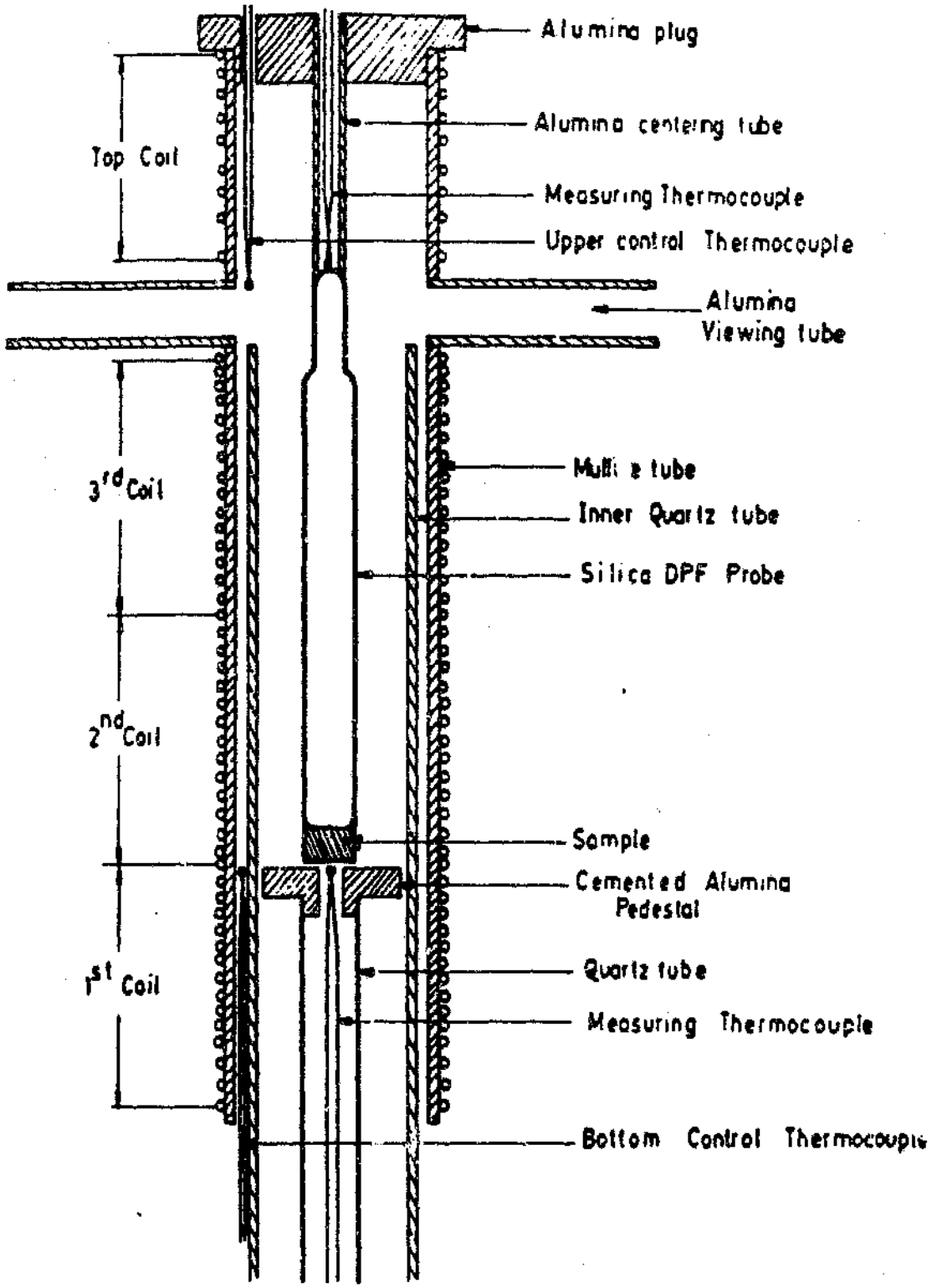


Figure 12. Part of the apparatus showing dew-point furnace, tube, windings, sample tube arrangement and the thermo- couples.

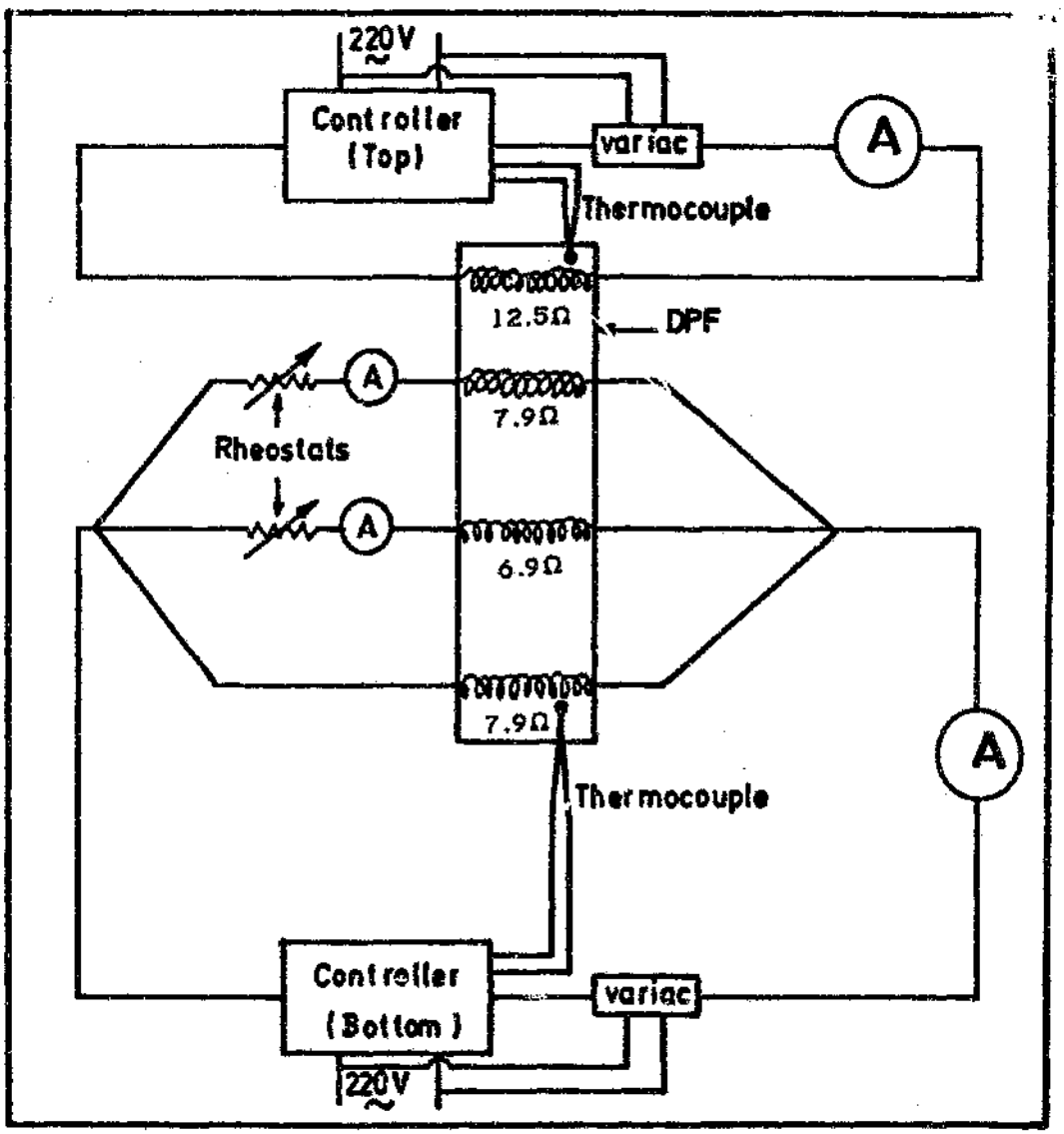


Figure 13. Schematic drawing of the electrical circuit of the dew-point furnace.

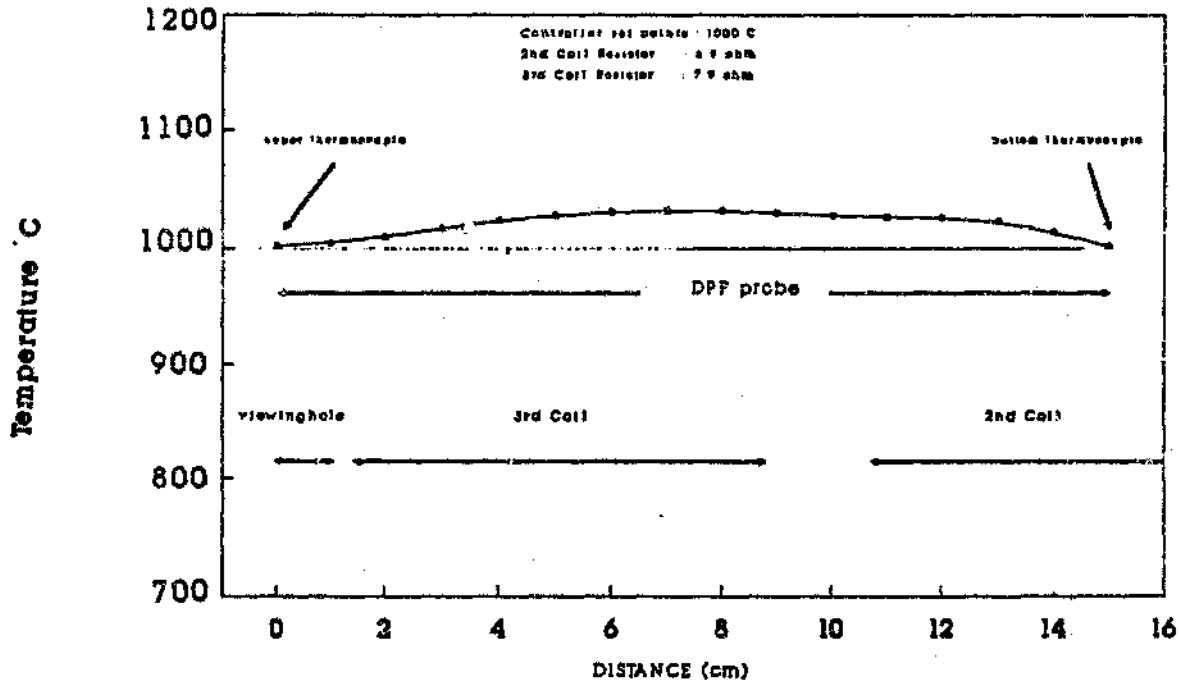


Figure 14. Typical temperature profile of the dew-point furnace.

3.4 PRINCIPLES OF DEW-POINT TECHNIQUE

The Dew-Point technique of activity measurements takes advantage of the volatility of a component in the solution under consideration. In this method the pressure of the volatile component over sample is determined from observations of the temperature at which condensation of the vapour occurs. This method is said to be most suitable when the vapour pressure of the components (in a binary system for example) would differ by at least three to two orders of magnitude[7].

For dew-point measurements, the sample being studied is placed in an evacuated and enclosed transparent silica tube. The tube is heated in DPF under a temperature gradient maintained between the bottom and the top of the tube at temperature T. The tube and its contents are heated for a sufficient period for a gaseous phase in equilibrium with the condensed phase at T to develope. The top of the tube is then cooled until condensation from the gas phase is observed. The temperature T_c at which the condensation occurs is called the dew-point of the volatile species. The vapour pressure of the condensing species above its pure reference condensed state at T_c is identical with the partial pressure of the condensing species above the condensed phase at T.

Temperatures at both ends of the silica tube are measured by thermocouples, and by repeated heating and cooling the dew-point temperature T_c can be determined accurately by observing the condensing particles through viewing holes to within ±1°C.

Once the dew-point temperature T_c is established, the

activity of the volatile component at T can be calculated from the following equation:

$$a_i = P_i(T_c)/P^\circ_i(T) \qquad (19)$$

Where $P_i(T_c)$ is the vapour pressure of component i at T_c, and $P^\circ_i(T)$ is the vapour pressure of i at T. Both $P_i(T_c)$ and $P^\circ_i(T)$ can be obtained from the vapour pressure equations of i available in literature. This method is quite efficient in that numerous activities of i can be determined in a single sample at various temperatures T by measuring the corresponding dew-point temperatures T_c.

3.5 PREPARATION OF DEW-POINT PROBES

Enclosed and evacuated transparent silica tubes containing the samples were used for dew-point measurements. In order to aviod the oxidation of metallic lead and other sulphide components the samples were argon flushed and evacuated in the following manner:

One end of a long transparent silica tube 10 mm in diameter was sealed with a hydrogen torch. A sample of desired composition, weighing about 5 grams was placed in the tube. The tube was narrowed with the torch at a distance of 15 cm from the closed end to form a nipple and neck. This distance was dictated by the temperature profile of the DPF. The silica tube was then connected to the Edwards E1M5 combined outfit vacuum system and evacuated to approximately 5×10^{-2} torr by means of the rotary pump. Commercially pure argon gas was allowed to flush the tube by means of a three-way stopcock connected to the vacuum system. This procedure of

evacuation followed by flushing was repeated twice for each sample. The gas train was then closed and the tube was evacuated to approximately 5 x 10^{-5} torr by using the diffusion pump. Finally, the tube was sealed at the neck under vacuum so that it was ready for use in the DPF.

3.6 MEASUREMENT OF DEW-POINT TEMPERATURE

The dew-point probes were gradually inserted into the DPF from the bottom slowly and was held in position on a cemented alumina pedestal supported by quartz tube. This pedestal served as a radiation shield. Through the inside of the quartz tube and a small hole in the centre of pedestal a Pt/Pt-13 % Rh thermocouple was inserted to measure the sample temperatures. The dew-point probe was centered by an alumina tube suspended from an alumina plug situated at the top of the DPF tube, so that the tip of the probe was clearly visible through the viewing hole. A second Pt/Pt-13 % Rh thermocouple was suspended through this alumina tube for the measurement of dew-point temperatures at the tip of the probe.

At the beginning of each experiment, both ends of the DPF was kept at the same temperature (1200°C) for approximately 16 hours (overnight) to ensure that equilibrium between the vapour and condensed phases has been reached[7]. Thereafter, by means of temperature control devices of the fourth coil, the tip of the probe was cooled gradually until small condensing particles were observed through a telescope directed at the tip of the probe from the alumina viewing tubes.

The condensate was re-evaporated and re-condensed several times while continuously decreasing the temperature interval of the super heating and cooling. This procedure allowed the determination of the dew-point temperatures of Pb and PbS, within ±4°C.

Upon completion of a dew-point experiment the probe was removed from the furnace. In all of the experiments, no reaction was observed between the liquid sample and the silica container. Furthermore, the tubes remained intact throughout each experimental run.

The dew-point procedure was applied to determine the PbS activities in FeS-PbS binary and Pb activities in Fe-Pb-S ternary systems.

3.7 PROCEDURE FOR QUENCHING EXPERIMENT

The classical equilibration - quenching technique was used to establish the equilibrium relations between immiscible melts of the Fe-Pb-S system and the position of the liquidus in the FeS-PbS binary system, which resulted in the construction of the FeS-PbS and Fe-Pb-S phase diagrams.

The distribution of the tie-lines in the ternary miscibility gap of the system Fe-Pb-S was ascertained by determining the compositions of sulphide saturated and sulphur saturated liquid phases which were in equilibrium with each other at 1200°C. The samples for this study were prepared by mixing elements Fe, Pb and S in such a manner that their gross composition would lie along the midrange of the miscibility gap. These samples, each weighing approximately 5 grams, were placed in silica tubes, each flushed with argon twice and evacuated to 5 x

10^{-5} torr. They were then sealed to a final length of 40 mm. These tubes were placed in alumina crucibles and suspended by a platinum wire into the vertical tube furnace. They were then heated at 1200°C for a period sufficient to affect the melting of the charge, its separation into two liquids, and the attainment of equilibrium between these liquids. The time taken to reach equilibrium was established in initial experiments by chemical analyses of stratified liquids at intervals of two hours for a total of eight hours. These analyses revealed that five hours would be sufficient for equilibrium to be achieved. Actual runs, however, were undertaken for at least six hours each for absolute certainty.

During equillibration, the sulphide rich and metal rich phases formed two liquids which were virtually immiscible in each other; the sulphide melt floated on top of the metal melt because of its lower density. This stratification was preserved when the samples were quenched to room temperature by carefully dropping the capsules into the water at the end of the equilibration run.

The quenched samples were removed from the capsules, the immiscible phases were separated readily from each other, and representative portions of these were analyzed chemically for their Fe, Pb and S contents in order to determine the boundaries of immiscibility region.

The position of the liquidus and eutectic line in the FeS-PbS binary within the temperature interval 800 - 1200°C were also determined by same technique as summarized above. Equilibration time for FeS-PbS system was determined to be about twelve hours and after attainment

of equilibrium the capsules were quenched to room temperature by carefully dropping them into cooled water. The samples were removed and representative portions were analyzed chemically, metallographically and by Energy Dispersive Analysis of X Rays (EDAX), where applicable. The position of the liquidus boundaries and eutectic line was established mainly by metallographic examination and EDAX. For metallography and EDAX, the specimens were mounted in liquid epoxy resin which permeated the pores and cracks of the sample before hardening. This greatly facilitated grinding and polishing.

Phase identifications were made with a reflected light microscope. Samples quenched from above the liquidus line showed no solid phases but only the quenched dendritic liquid. On the other hand, samples quenched from below the liquidus curve showed the two phase region. Metallographic examination of such samples revealed the existence of small globules of solid phase embedded in matrix of dendritic quenched liquid.

The error estimation for EDAX analyses are as follows:

S: less than 0.07 wt %
Fe: less than 0.7 wt %
Pb: less than 0.3 wt %

3.8 CHEMICAL ANALYSES PROCEDURE

Chemical analyses for iron, lead and sulphur were performed at Mintek to determine the compositions of the samples obtained from quenching and occasionally from dew-point experiments.

For iron and lead determination; the sample was fused in Na_2O and leached in water, then acidified. An internal standard (scandium) was added and then made to volume. The weight percentages of the elements were then determined using emission spectroscopy with an inductively coupled plasma source. The estimated error in respect of lead and iron determination was less than 5%.

The amount of sulphur was established by using a LECO Sulphur determinator. This apparatus operates by burning the sulphur while passing oxygen over the sample so that SO_2 is formed. This gas is collected and filtrated by iodine and the sulphur content of the sample is directly read from the instrument. The estimated error of sulphur determination was reported to be less than 1%.

For stoichiometric FeS-PbS solutions the analysis for the elements namely Fe, Pb and S totalled 99.4 ± 0.8 %. These were corrected slightly to make the total 100 % from which compositions of stoichiometric species FeS and PbS were calculated. It was observed that the calculated compositions for these species after experiments were within 1 % of the starting compositions. Furthermore, the analysis for PbS corresponded to the stoichiometric formula and that for FeS yielded $FeS_{1.011}$.

4. EXPERIMENTAL RESULTS AND DISCUSSION

The experimental results of this study are presented in two sections: (1) Results on phases present at the equilibration temperatures in the system FeS-PbS, and compositions of co-existing liquids at 1200°C in the system Fe-Pb-S are given in the section of "Phase Equilibria". (2) The results of measurements on dew-point temperatures for FeS-PbS system and activity calculations of Fe-Pb-S systems are presented both in tabular and graphical forms in the section "Thermodynamics".

4.1 PHASE EQUILIBRIA

4.1.1 PRESENTATION OF RESULTS IN FeS-PbS SYSTEM

The phases present in various samples of the FeS-PbS system at the equilibration temperatures as identified by the methods discussed earlier, are listed in Tables 1a and 1b. These data were obtained mainly with the purpose of delineating the liquidus lines, eutectic temperature, and solubility curves.

The results given in Tables 1a and 1b are summarized in Figure 15 showing the position of the liquidus, solid solubility curves and the eutectic line.

Occasionally chemical analyses were performed on equilibrated samples to check whether the overall composition of the samples have changed or not. The chemical analyses confirmed that the samples have kept their stoichiometric compositions within the error limits of the chemical analyses.

It is well known that FeS is a non-stoichiometric compound with the actual formula $Fe_{1-x}S$ or FeS_{1+y}. However, the homogeneity range is very narrow and is a function of sulphur partial pressure. In the present case pure iron sulphide prepared by the method described earlier when analyzed for its iron and sulphur contents (63.28% Fe and 36.72% S) yielded the chemical formula $FeS_{1.01}$.

Table 1a; Experimental data of Quenching Experiments on FeS-PbS Binary system.

Sample composition (Mole Fraction)		Equilibrium Temperatures	Phase Identified
X_{PbS}	X_{FeS}	T °C	
0.07	0.93	1125	solid+liquid
0.15	0.85	1125	liquid
0.17	0.83	1050	solid+liquid
0.25	0.75	1050	liquid
0.27	0.72	975	solid+liquid
0.35	0.65	975	liquid
0.36	0.64	885	solid+liquid
0.46	0.54	885	liquid
0.57	0.43	885	solid+liquid
0.62	0.38	975	liquid
0.72	0.28	975	solid+liquid
0.79	0.21	1050	liquid
0.88	0.12	1050	solid+liquid
0.26	0.74	845	solid+liquid
0.26	0.74	839	solid1+solid2

Table 1b; SEM EDAX Results of Quenching Experiments on the two-solid region of the FeS-PbS Binary System

Sample composition (Mole Fraction)		Equilibrium Temperature	SEM EDAX results of identified solid phases	
X_{PbS}	X_{FeS}	T °C	X_{PbS}	X_{FeS}
0.07	0.93	1125	$3x10^{-4}$*	0.9997*
0.27	0.73	1050	$9x10^{-4}$*	0.9991*
0.36	0.64	885	$1.4x10^{-3}$*	0.9986*
0.26	0.74	795	$2x10^{-4}$*	0.9998*
0.72	0.28	1050	0.9992**	$8x10^{-4}$**
0.57	0.43	975	0.9996**	$4x10^{-4}$**
0.26	0.74	795	0.99997**	$3x10^{-5}$**

* FeS rich solution

** Pbf rich solucion

Therefore in all the presentations and calculations, iron sulphide was assumed to be stoichiometric FeS.

SEM-EDAX analyses of solid phases in the equilibrated samples, data of which is collected in Table 1b, have permitted the construction of solid solubility at both ends of the diagram. In reality the solid phases were micro-analyzed by SEM-EDAX for their lead, iron and sulphur contents. In general, the analyses for the chemical constituents totalled 99.4 ± 0.8%. These were normalized to 100% and converted to stoichiometric mole fractions of PbS and FeS. In these calculations an excess or deficiency of sulphur was not encountered within the error limits of microanalyses. This is a further proof of the soundness of the experimental results.

4.1.2. DISCUSSION OF RESULTS IN FeS-PbS SYSTEM

The phase diagram of FeS-PbS binary system was constructed both by experiments and mathematical modelling of the activity data, to be presented later. Eutectic temperature of FeS-PbS system was found as 842°C and eutectic composition was obtained at X_{PbS} = 0.46 by extrapolation of two liquid boundary curves, obtained from mathematical modelling of the liquidus curves. The experimental points lie at both sides of the calculated liquidus lines, confirming the soundness of the solution model. The melting points of both components were obtained from literature[16.17].

The solid solubility of each component in each other, as can be seen from Table 1a is very small and for practical purposes negligible.

The general shape of the phase diagram constructed in this investigation is slightly different when compared with the published diagram of Kerby[3] and Brett[4]. Kerby's eutectic line is slightly lower than the present study, indicating a eutectic temperature of 835°C at X_{PbS} = 0.48. However, Brett[4] found a eutectic temperature Te=848°C which is higher than the present study.

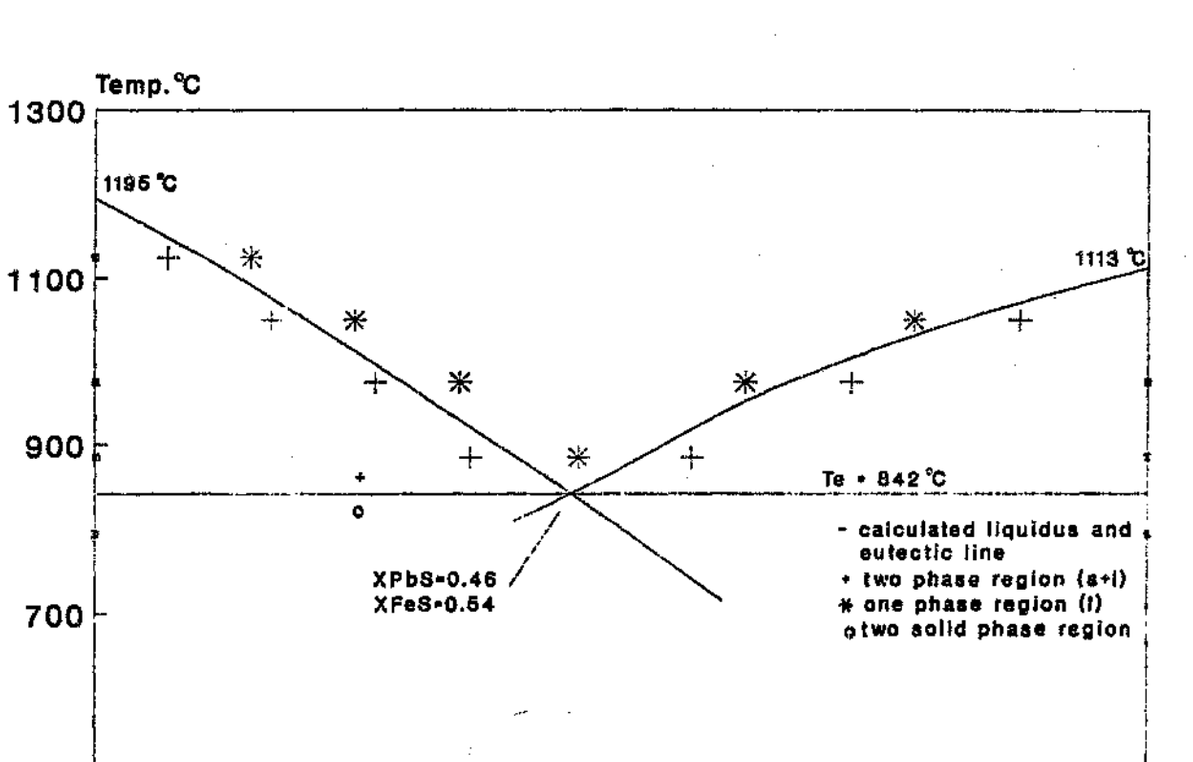


Figure 15. FeS-PbS phase diagram of the present study.

4.1.3. PRESENTATION OF RESULTS IN Fe-Pb-S SYSTEM

In the Fe-Pb-S ternary system, the region of greatest metallurgical interest is that bounded by the compositions Fe-FeS-PbS-Pb. Within this field a ternary liquid immiscibility gap exists at 1200°C. Tie-lines joining the equilibrium compositions of co-existing sulphur rich and metal rich liquid phases were determined at 1200°C by the method described in section (3.7) and the boundaries of liquid immiscibility were redrawn based on the compositions of the end points of the tie-lines. Compositions of the region $Fe_\gamma + L_1$ in Fe-FeS side and $Fe_\gamma + Pb_{(l)}$ in Fe-Pb side were taken from both binary diagrams available in literature[11,12]. The relevant data are given in Table 2 and Figure 16 is a graphical summary of the results.

In Figure 16 the full circles represent the end-points of the tie-lines. The heavy lines represent the boundaries of the miscibility gap derived from the tie-line data. The heavy straight line joining the compositions FeS and PbS represents stoichiometric FeS-PbS liquid solutions and is hypothetical.

Table 2; Experimental data on Tie-lines of the Fe-Pb-S system at 1200°C

Tie Line Number	Compositions (mole fraction)					
	Along metal rich boundary			Along sulphur rich boundary		
	X_{Fe}	X_{Pb}	X_S	X_{Fe}	X_{Pb}	X_S
1	0.002	0.993	0.005	0.585	0.015	0.400
2	0.013	0.970	0.017	0.550	0.038	0.412
3	0.014	0.961	0.025	0.510	0.060	0.430
4	0.014	0.945	0.041	0.470	0.090	0.440
5	0.014	0.930	0.056	0.430	0.101	0.469
6	0.016	0.912	0.072	0.390	0.140	0.470
7	0.018	0.908	0.073	0.352	0.168	0.480
8	0.023	0.865	0.112	0.305	0.210	0.485
9	0.021	0.844	0.135	0.256	0.255	0.490
10	0.023	0.82	0.157	0.199	0.308	0.493
11	0.033	0.73	0.237	0.125	0.390	0.485

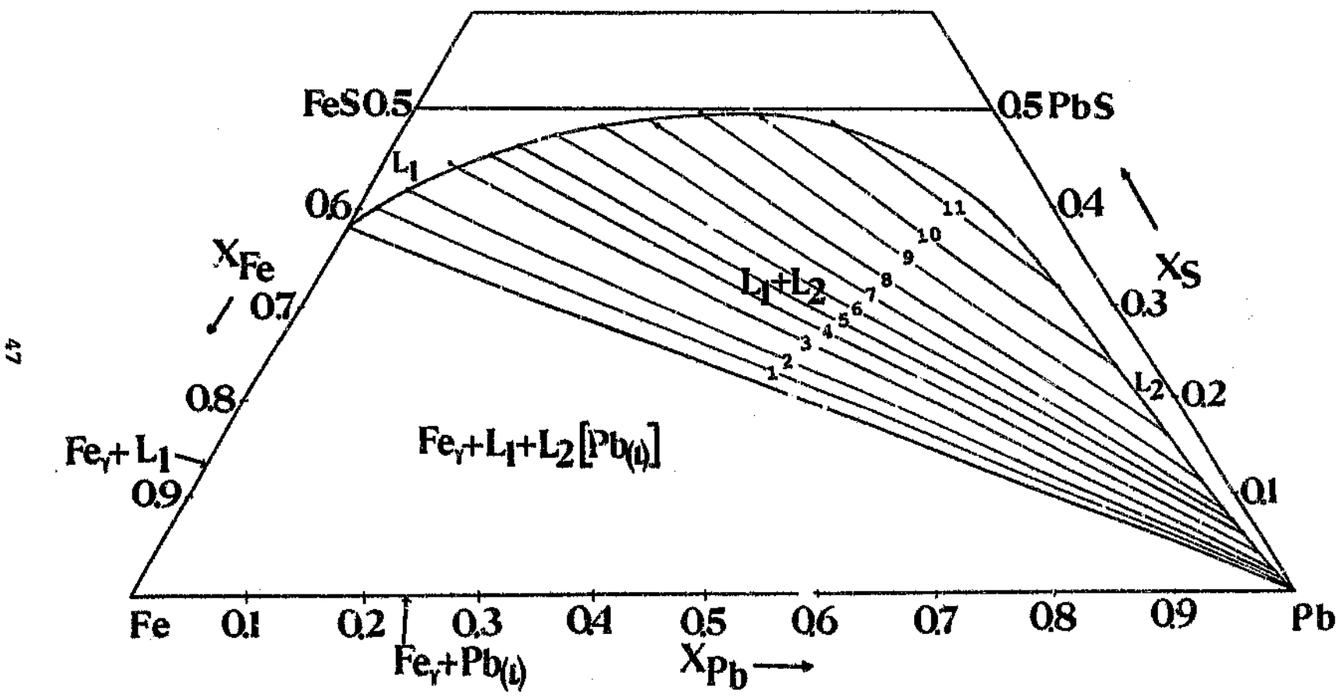


Figure 16. Experimentally determined tie-lines in Fe-Pb-S melts at 1200°C

4.1.4. DISCUSSIONS OF RESULTS IN Fe-Pb-S SYSTEM

In literature there is no comparable ternary isothermal section of the Fe-Pb-S diagram at 1200°C. Therefore, this is the first study revealing phase relations in this system at 1200°C. However, the liquidus projection of Fe-Pb-S system available in literature, although based on extrapolations rather than experimental findings, predicts a small ternary immiscibility region which is in accord with the present findings. This region as shown in Figure 7 was the starting point for this investigation during quenching experiments in Fe-Pb-S system.

The distribution of tie-lines at 1200°C in the ternary immiscibility gap, illustrated in Figure 16, cover the whole composition range between the straight line, separating the two liquid region from the three phase region, drawn from the Fe-FeS side (X_{Fe}=0.62) to Pb corner, and upper boundary towards PbS corner. This line was drawn by the use of information available in literature[11]. A sample whose composition was just below and at about midpoint of the straight line joining X_{Fe}=0.62 to Pb corner, after equilibration and examination following quenching, revealed the three phases (primary solid Fe-γ and two liquids) confirming the extent of immiscibility. The direction of tie-lines are closely related to the soundness of chemical analyses. Especially at sulphide saturation regions of the miscibility gap, small errors in the analyses may result in different orientations of tie-lines. In order to minimize the errors, chemical analyses has been done twice for each sample and an average composition value has been taken to position the end points of each tie-line. In subsequent thermodynamic

calculations, the end points of tie-lines were directly read from the boundary curves.

4.2 THERMODYNAMICS

The activity measurements in FeS-PbS melts were carried out by the dew-point technique at 1100 and 1200°C. The activities of Pb at 1200°C were also measured by the dew point technique in samples selected from the lead-rich ends of the previously determined tie lines. The activities of iron, sulphur, as well as lead itself were calculated employing the tie-line data and binary thermodynamic information.

4.2.1. PRESENTATION OF RESULTS IN FeS-PbS SYSTEM

PbS activities of the binary FeS-PbS liquid samples at 1200°C, 1100°C were determined by the dew-point technique described earlier in sections (3.4, 3.6). Equations 2 and 3, giving the vapour pressure of solid and liquid PbS respectively as a function of temperature was employed to convert the measured dew-point temperature into activity values. The dew-point temperatures of selected FeS-PbS samples were inserted into equation 2 or 3 and thus the ratio of calculated partial pressure of PbS (P_{PbS}) to the vapour pressure of pure liquid PbS (P°_{PbS}) gave the required activities with pure liquid PbS as the standard state from the following:

$$a_{PbS} = P_{PbS}/P^{\circ}_{PbS} \qquad (20)$$

Upon completion of a dew-point run the silica tube was quenched in air and the sample was removed for phase identification and occasional chemical analyses. Microscopic examination of samples revealed the existence of one phase only in all the samples studied at each temperature This is in accord with the redrawn FeS-PbS phase diagram. The occasional chemical analyses for iron, lead and sulphur content of the samples revealed that there was no change in the composition of the samples within analytical error limits. The relevant data covering the compositions, dew point temperatures with their error ranges and activities are collected in Table 3 and Figure 17, all of which also include calculated PbS and FeS activities through Krupkowski formalism.

To calculate activity of a species in a solution α function may be used. The α function for a species is defined as follows;

$$\alpha_i = \ln \gamma_i/(1-X_i)^2 \qquad (21)$$

where γ_i is the activity coefficient ($a_i = \gamma_i X_i$) and X_i is the mole fraction of species "i". Since the α function for PbS derived from the experimental activity data did not show linear behaviour with composition, the regular solution models could not be applied for this system. After trying other solution models, it has been found that Krupkowksi formalism could well describe the FeS-PbS system, which showed negative deviation from Raoult's Law.

Krupkowski[33] has employed the following formulae for binary solutions:

$$\ln\gamma_1 = W(T)\,(1-X_1)^n \qquad (22)$$

$$\ln\gamma_2 = W(T)\left[(1-X_1)^m - \frac{m}{m-1}(1-X_1)^{m-1} + \frac{1}{m-1}\right] \qquad (23)$$

Equation 23 is derived from the Gibbs-Duhem equation ($x_1 d\ln\gamma_1 + x_2 d\ln\gamma_2 = 0$) assuming that equation 22 applies for component 1. The function W(T) and parameter m must be determined from experimental data. As indicated by equation 22, the exponent m can be obtained from the slope of a plot of $\ln(\ln\gamma_1)$ vs $\ln(1-x_1)$; the intercept yields ln W(T), or once m is fixed W(T) can be calculated from equation 22. Over a limited temperature range, m is usually but not necessarily independent of temperature. Such a procedure generally applies for systems with positive deviations from Raoult's Law and then the parameter m, which is called the assymmetry coefficient, takes the values $1<m<2$. The closer m is to unity, the greater the assymetry of the thermodynamic functions.

Moser[34] has shown that the values of $m>2$ appear in systems with negative deviations from ideality and in the case of such systems $W(T)<0$. The function W(T) is temperature dependent and for many systems takes the form $A/T - B$.

With the application of the formalism to the experimentally determined PbS activities in FeS-PbS binary system, the intercept ; W(T) and slope ; m values were calculated from the plot of $\ln(-\ln\gamma_{PbS})$ vs $\ln(1-x_{PbS})$ as ; W(T) = -1.034, m = 2.4 at 1200°C and W(T) = -1.402, m = 2.031 at 1100°C after relevant regression analyses with a correlation factor of 0.98.

Therefore, $\ln\gamma_{PbS}$ and $\ln a_{PbS}$ at 1200°C can be expressed as:

$$\ln\gamma_{PbS} = -1.034(1-X_{PbS})^{2.4} \quad (24)$$

$$\ln a_{PbS} = \ln X_{PbS} - 1.034(1-X_{PbS})^{2.4} \quad (25)$$

The corresponding $\ln\gamma_{FeS}$ and $\ln a_{FeS}$ could then easily be obtained:

$$\ln\gamma_{FeS} = -1.034[(X_{FeS})^{2.4} - 1.71(X_{FeS})^{1.4} + 0.714] \quad (26)$$

$$\ln a_{FeS} = \ln X_{FeS} - 1.034[(X_{FeS})^{2.4} - 1.71(X_{FeS})^{1.4} + 0.714] \quad (27)$$

By using the same procedure $\ln a_{PbS}$ and $\ln a_{FeS}$ at 1100°C can be expressed as:

$$\ln a_{PbS} = \ln X_{PbS} - 1.402(1-X_{PbS})^{2.031} \quad (28)$$

$$\ln a_{FeS} = \ln X_{FeS} - 1.402[(X_{FeS})^{2.031} - 1.97(X_{FeS})^{1.031} + 0.97] \quad (29)$$

The last two columns of Table 3 also contain calculated activity values from equations 25, 27, 28 and 29 at 1200°C and 1100°C respectively for comparison with experimentally measured values. In figure 17, the full lines represent the activities calculated by model equations.

By applying the equation 7, which gives the activity of PbS in equilibrium with solid PbS, it was possible to derive the liquidus temperature of PbS analytically.

Table 3a; Data on Dew-Point temperatures and results of activity calculations in FeS-PbS system at 1200°C.

Sample composition (Mole Fraction)		Measured Dew-Point Temperatures	Experimental Activities of PbS	Activities Calculated by Model	
X_{PbS}	X_{FeS}	T °C	a_{PbS}	a_{PbS}	a_{FeS}
0.1	0.9	1071 ± 3.0	0.042	0.045	0.889
0.2	0.8	1030.2 ± 3.0	0.118	0.109	0.763
0.3	0.7	1065.0 ± 3.0	0.204	0.193	0.632
0.4	0.6	1090.0 ± 3.0	0.293	0.295	0.504
0.5	0.5	1110.1 ± 4.0	0.396	0.411	0.384
0.6	0.4	1142.0 ± 3.0	0.532	0.535	0.279
0.7	0.3	1159.9 ± 3.0	0.669	0.661	0.188
0.8	0.2	1174.5 ± 3.0	0.780	0.783	0.113
0.9	0.1	1189.1 ± 3.0	0.897	0.896	0.051

Table 3b; Data on Dew-Point temperatures and results of activity calculations in FeS-PbS system at 1100°C.

Sample composition Mole Fraction		Measured Dew-Point Temperatures	Experimental Activities of PbS	Activities Calculated by Model	
X_{PbS}	X_{FeS}	T °C	a_{PbS}	a_{PbS}	a_{FeS}
0.1*	0.9*	-	-	-	-
0.2	0.8	944.0 ± 3.0	0.081	0.082	0.756
0.3	0.7	973.2 ± 3.0	0.135	0.152	0.616
0.4	0.6	1009.2 ± 3.0	0.249	0.243	0.479
0.5	0.5	1032.0 ± 4.0	0.358	0.355	0.352
0.6	0.4	1054.1 ± 3.0	0.486	0.482	0.242
0.7	0.3	1067.4 ± 3.0	0.622	0.620	0.152
0.8	0.2	1081.5 ± 2.5	0.766	0.770	0.082
0.9	0.1	1091.6 ± 3.0	0.886	0.888	0.033

* solid + liquid phase region

Combining equation 7 with equation 25 and solving for temperature T, the position of the PbS liquidus was obtained. This is possible only when it is assumed that no solid solubility exists. Since the experimentally found solid solubilities at both ends of the diagram were very small, they were neglected in liquidus temperature calculations.

In a similar way by combining equation 18 with equation 27 and solving for Temperature T, the position of the FeS liquidus was obtained with, again, no solid solubility assumption.

The solid lines in Figure 15 represent the calculated liquidus curves as explained above. The intersection of two liquidus curves, that for FeS and PbS, yielded the eutectic temperature of 842°C and its composition at X_{PbS}=0.46.

Henrian activity coefficient for both PbS and FeS can be calculated from equations 24 and 26 at 1200°C when the appropriate mole fractions tend to zero as γ°_{PbS}=0.356 and γ°_{FeS}=0.478.

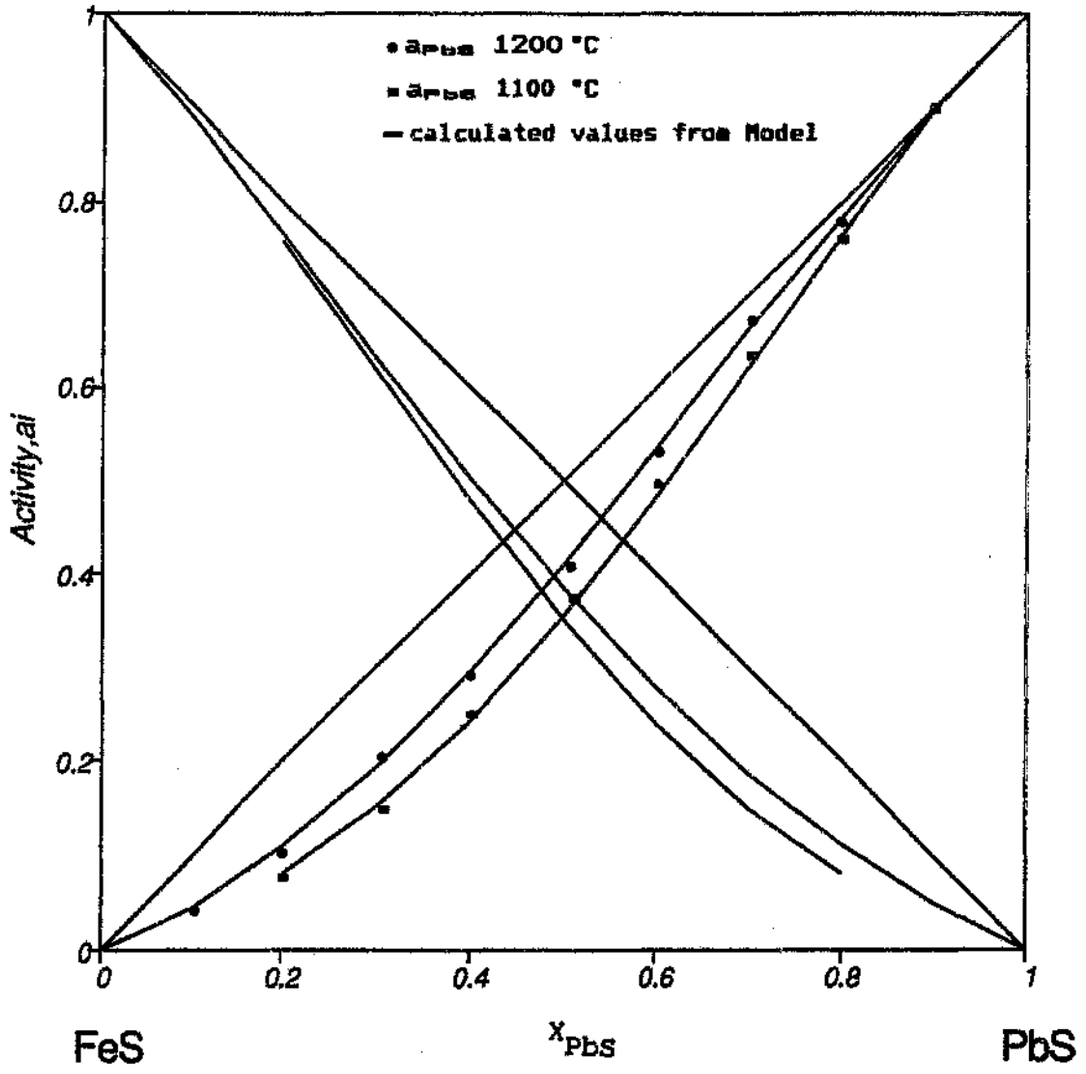


Figure 17. FeS-PbS Activity curves of present study

4.2.2 DISCUSSION OF RESULTS IN FeS-PbS SYSTEM

Activities of both components of the FeS-PbS system show moderate negative departures from ideality in accord with an experimentally determined phase diagram, as shown in Figure 17.

Nesterov[19] measured the vapor pressures of PbS by the transpiration method over FeS-PbS melts in the range 1000 - 1250°C: the PbS activities were observed to exhibit negative behaviour from ideality, as reproduced in Figure 9. These data, however, covered only a limited composition range, $X_{PbS} \leq 0.35$, and hence were insufficient to derive information on the activities of FeS. On the other hand, the activity calculation of Eriç[18] based on the data obtained by the dew-point technique in the same system showed ideal behaviour for both PbS and FeS activities. However, they reported the necessity of a reinvestigation of phase relations in the system because of the anomaly observed in PbS activities obtained from the PbS branch of liquidus.

An analysis of the errors involved in using the dew-point method of activity determination has been made by Eriç[24] and Birchenall and Cheng[25]. The largest source of error is an incorrect measurement of the dew-point temperature. This reproducibility of the dew-point temperatures in the FeS-PbS system changed from 1 to 4°C at 1200°C. Hence, starting from the highest value, the maximum error in a measured PbS activity can be estimated as follows: The temperature coefficient of PbS vapour pressure for pure PbS at 1200°C from equation 3 is $dP/dT = 2.72\ 10^{-3}$ atm/K. Therefore a maximum error of 4°C in dew-point temperature corresponds to an error of

$\Delta P^{\circ}_{PbS} = 1.1 \times 10^{-2}$ atm in measuring the value $P^{\circ}_{PbS} = 0.281$ atm for pure PbS. For this particular sample with maximum error, the activity is 0.396 and the equilibrium vapour pressure is $P_{PbS} = 0.111$ atm. The error in this P_{PbS} results in $\Delta P_{PbS} = 4.8 \times 10^{-3}$ atm. The absolute error in the activity is related to the relative errors in pressures by the following equation[24]:

$$\Delta a_i / a_i = (P_i^{\circ} \Delta P_i - P_i \Delta P_i^{\circ}) / (P_i (P_i^{\circ} + \Delta P_i^{\circ})) \qquad (30)$$

By inserting $\Delta P^{\circ}_{PbS}, P_{PbS}, \Delta P_{PbS}, P^{\circ}_{PbS}$ values calculated above into equation 30, the absolute percentage error in determining $a_{PbS} = 0.396$ for this particular sample becomes 0.39%. By using the same method, in determining $a_{PbS} = 0.358$ at 1100°C, becomes 0.47%.

The accuracy improves further for samples with less uncertainty in their measured dew-point temperatures. Thus it can be concluded that the effect of uncertainties in dew-point temperatures to the reported activities are negligible.

The second source of error in dew-point measurements is the change of the original sample composition due to PbS vaporization into the specimen tube. In this study this type of error was also negligible, since it was calculated from the ideal gas equation that at 1200°C 6.55 mg of PbS, and at 1100°C 2.38 mg of PbS would be sufficient to maintain the equilibrium lead sulphide vapour pressure over a sample of pure PbS. 6.55 mg of PbS represents the highest amount of PbS in the vapour phase among all samples. The total weight of the specimen in each run was approximately

5 to 6 grams, hence the PbS removed by vaporization would not cause a significant change in the original composition of the specimen. The changes in sample composition due to PbS condensates at the tip of the dew-point probe were also neglible, because the few that were formed were also very small.

4.2.3 PRESENTATION AND DISCUSSIONS OF RESULTS IN Fe-Pb-S SYSTEM

Activities in Fe-Pb-S ternary system were evaluated by two different methods, both of which are based on the Gibbs-Duhem relation. Firstly, by using the method developed by Choudary and Chang[26, 27], activities of iron, lead and sulphur were calculated from the experimentally determined tie-lines along the miscibility gap of the Fe-Pb-S ternary system . Secondly, by ternary Gibbs-Duhem integration, Fe and S activities were calculated using experimentally measured Pb activities of samples selected from the lead-rich ends of the experimentally determined tie-lines. These methods are as follows:

i) Activity calculations by the method of Choudary and Chang[26, 27]:

At constant temperature T, and pressure P, the generalized Gibbs-Duhem relation is:

$$\sum n_i d\bar{Q}_i = 0 \qquad (31)$$

where n_i's refer to the number of moles of the component and Q_i is any partial molar thermodynamic property of the ith component. Following Chipman[28],

the concentration variable n_i is changed to the new concentration variable y_i, henceforth referred to as the "atom ratio" of component i. The definitions of the atom ratios in ternary A-B-C system where A and B are metals and C is a non-metal, are given below:

$$y_A=n_A/(n_A+n_B)=1-y_B \qquad (32a)$$

$$y_B=n_B/(n_A+n_B) \qquad (32b)$$

$$y_C=n_C/(n_A+n_B) \qquad (32c)$$

Expressing equation 31 in terms of activity coefficients and substituting n_i by y_i from equations 32 yields:

$$y_A d\ln\gamma_A+y_B d\ln\gamma_B+y_C d\ln\gamma_C=0 \qquad (33)$$

Figure 18 shows lines of constant y_C and y_A (or y_B), the miscibility gap along which equation 33 is to be integrated and the composition notations. $y_C=0$ shows metallic A-B binary; $y_i = y_i^*$ shows compositions of non-metal saturated metallic phases in equilibrium with metal poor phases denoted by $y_i = y_i'$.

From equation 33 and following Wagner[29] an important relation was developed by Choundary and Chang[26,27], expressing the variation of $\ln(\gamma_B/\gamma_A)$ with y_C^* in terms of the change of $\ln\gamma_C$ with y_B. Knowing the tie line-distribution in the two liquid phase and the boundary binary thermodynamics, this relationship may be utilized to compute all the pertinent thermodynamic data along the miscibility gap.

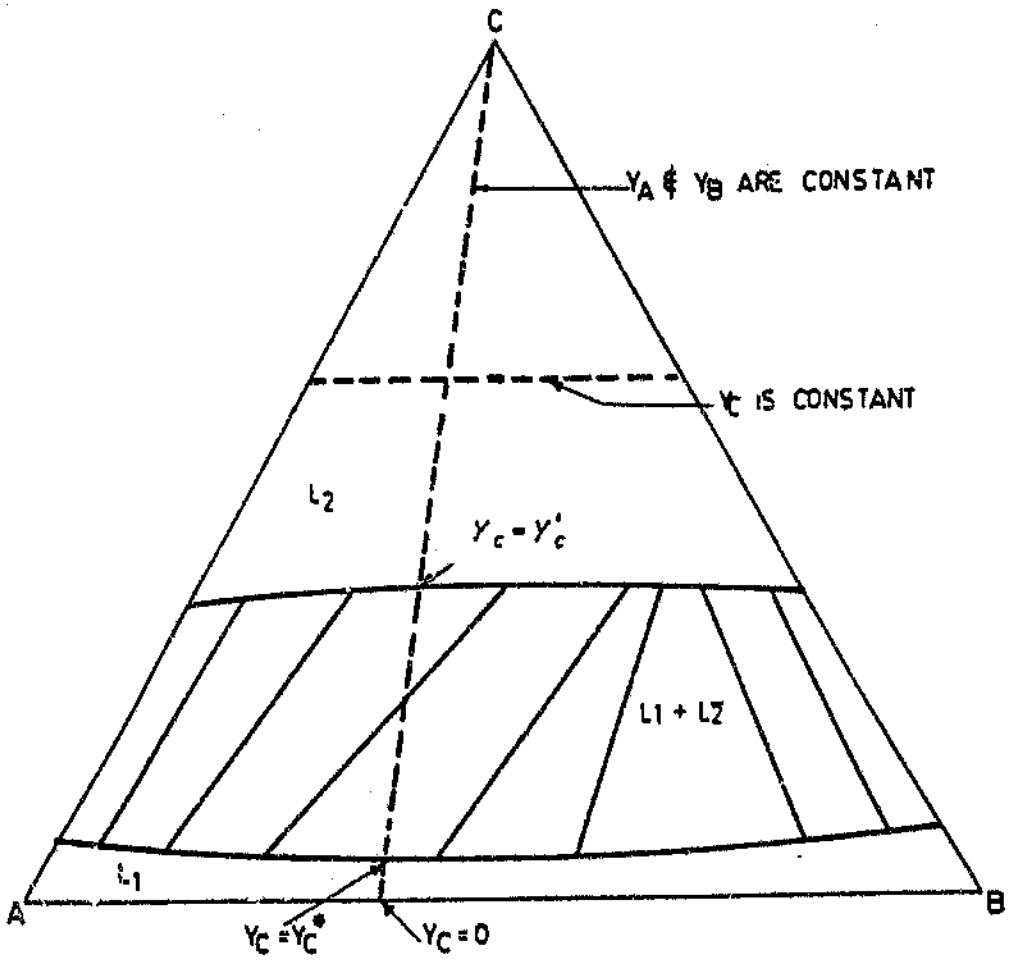


Figure 18. Schematic of an isothermal section showing a miscibility gap in a ternary system A-B-C.

In derivation of this new equation y_B and y_C are independent variables with $y_A = 1 - y_B$. Thus from equation 33 the following relations are written:

$$(1-y_B)\left(\frac{d\ln\gamma_A}{dy_B}\right)+y_B\left(\frac{d\ln\gamma_B}{dy_B}\right)+y_C\left(\frac{d\ln\gamma_C}{dy_B}\right)=0 \qquad (34)$$

$$(1-y_B)\left(\frac{d\ln\gamma_A}{dy_C}\right)+y_B\left(\frac{d\ln\gamma_B}{dy_C}\right)+y_C\left(\frac{d\ln\gamma_C}{dy_C}\right)=0 \qquad (35)$$

Differentiation of equations 34 and 35 with respect to y_C and y_B, and upon subtraction and subsequent rearrangement of the terms yields the following important relationship[26,27]:

$$\left(\frac{d\ln(\gamma_B/\gamma_A)}{dy_C}\right)=\left(\frac{d\ln\gamma_C}{dy_B}\right) \qquad (36)$$

Integrating equation 36 from $y_C=0$ to $y_C=y_C^*$ along constant y_A and y_B yields the following equation for $\ln(\gamma_B/\gamma_A)$ along the metal-rich miscibility gap boundary as

$$\left(\ln\frac{\gamma_B}{\gamma_A}\right)_{\left(\frac{y_B}{y_C=y_C^*}\right)}=\left(\ln\frac{\gamma_B}{\gamma_A}\right)_{\left(\frac{y_B}{y_C=0}\right)}+y_C^*\left(\frac{d\ln\gamma_C^*}{dy_B}\right)_{(y_B)} \qquad (37)$$

Where γ^*_C is the limiting activity coefficient of C at infinite dilution in A-B solutions. Equation (37) is strictly valid only if the variation $(d\ln\gamma_C/dy_B)$ with y_C is constant in the compositional range $0<y_C<y_C^*$. This is a reasonable approximation provided that the metal rich boundary of the miscibility gap lies close to the binary A-B. Thus the ratios of the activity coefficient and activities of B and A may be readily obtained from

equation (37) by utilizing the thermodynamic properties of the binary A-B and the limiting thermodynamic properties of C in the binary A-B.

Knowing the ratios of activity coefficients of B and A along the metal rich miscibility gap boundary as a function of metal atom ratio from equation (37), it is possible to calculate the activities of all three components by utilizing tie-line distribution data, through the following relations for coexisting liquid phases in the miscibility gap:

$$(1-y_B^*)\,dlna_A+y_B^*dlna_B+y_C^*dlna_C=0 \qquad (38a)$$

$$(1-y_B')\,dlna_A+y_B'dlna_B+y_C'dlna_C=0 \qquad (38b)$$

Subtracting equation (38b) from equation (38a) and rearranging the terms yield:

$$d(lna_C)_{y_B} = \left(\frac{y_B^*-y_B'}{y_C'-y_C^*}\right) dln(a_B/a_A)_{y_B} \qquad (39)$$

Multiplying equation (38a) by y_C' and (38b) by y_C^* and upon subtraction and rearrangement of terms yield a relation for the activity of A as:

$$d(lna_A)_{y_B} = \left(\frac{y_B'y_C^*-y_B^*y_C'}{y_C'-y_C^*}\right) dln(a_B/a_A)_{y_B} \qquad (40)$$

In the calculation of activities in Fe-Pb-S system equations (37), (39), and (40) were used with A for

lead, B for sulphur, and C for iron. Due to end points of the experimentally found tie lines being closer to the Pb-PbS boundary, it was decided to use the activity data from this boundary. Therefore the above mentioned equations were adopted to these data. Since the experimental values for the limiting activity-coefficient of iron in lead-sulphur melts were not available, they were calculated from the quasichemical relation of Jacob and Jeffes[30].

$$\ln\gamma^{\circ}_{Fe(Pb-S)} = y_{Pb}\ln\gamma^{\circ}_{Fe(Pb)} + y_S\ln\gamma^{\circ}_{Fe(S)} - \frac{2H^M}{RT} \qquad (41)$$

Where H^M is the enthalpy of mixing for the Pb-S solutions. With the quasichemical relationship of Jacob and Jeffes[30], equation (37) for Fe-Pb-S system takes the following form when expressed for activities[27].

$$\ln\left(\frac{a_S}{a_{Pb}}\right)_{\left(\frac{y_S}{y_{Fe}=y^{\circ}_{Fe}}\right)} = \left(\ln\frac{\gamma_S}{\gamma_{Pb}}\right)_{\left(\frac{y_S}{y_{Fe}=0}\right)} + \left(\ln\frac{y_S}{y_{Pb}}\right) + y^{\circ}_{Fe}\left[\ln\frac{(\gamma^{\circ}_{Fe(S)})}{(\gamma^{\circ}_{Fe(Pb)})} + \frac{2}{RT}\frac{(H^M - H^M_S)}{(1-y_S)}\right] \qquad (42)$$

The term H^M_S in the above relation represents the relative partial molar enthalpy of S in binary Pb-S solutions. The thermodynamic properties of Pb-S solutions, namely H^M and H^M_S as a function of composition were calculated with the use of data from Eriç[7].

H.A. Wriedt[31] has developed a method of calculation of activities in binary systems having miscibility gaps. To make these calculations, it is assumed that the function α_i defined in terms of activity coefficients, $\gamma_i = a_i/x_i$, and atom or mole fractions by the equation:

$$\alpha_i = \ln \gamma_i / (1-x_i)^2 \qquad (43)$$

is linear with composition, that is:

$$\alpha_2 = A + BX_1 = A + B(1-X_2) \qquad (44)$$

and by integration of binary Gibbs-Duhem equation,

$$\alpha_1 = A + B(1/2 + X_1) = A + B(3/2 - X_2) \qquad (45)$$

In essence, the above assumption of linearity of α_i function is identical with the sub-regular solution model developed by Hardy[32]. In sub-regular solutions the integral and partial molar free energies are expressed by two constant equations[32] as well.

The calculation of unkowns A and B expressed by Wriedt[31] as:

$$A = \frac{B}{2}(2X_2^{12} + X_2^{11} - 3) + \frac{1}{(X_2^{12} - X_2^{11})^2}\left[(1-X_2^{11}) \ln \left(\frac{1-X_2^{11}}{1-X_2^{12}}\right) + X_2^{11} \ln \left(\frac{X_2^{11}}{X_2^{12}}\right)\right] \qquad (46)$$

and

$$B = \frac{2}{(X_2^{11} - X_2^{12})^3}\left[2\ln\left(\frac{1-X_2^{11}}{1-X_2^{12}}\right) + (X_2^{11} + X_2^{12}) * \ln\left(\frac{X_2^{11}(1-X_2^{12})}{X_2^{12}(1-X_2^{11})}\right)\right] \qquad (47)$$

It was shown[31] that for symmetrical and wide gaps the activities calculated by the above equations were in excellent agreement with available experimental data.

Since the miscibility gaps in both Fe-S (on the FeS-S side) and Fe-Pb binary systems were very wide, it was decided to use equations of Wriedt[31] to calculate Henrian activity coefficient of iron at infinite dilution in liquid sulphur and in liquid lead at 1200°C respectively. At this temperature, the compositions of the two liquids in equilibrium in the Fe-S system were established as $X_S = 0.605$ and $X_S = 0.994$ (Fig 4.). Hence, the values of A and B were evaluated to yield the following α_{Fe} function.

$$\alpha_{Fe}=15.06-30.07(1/2+X_{Fe}) \qquad (48)$$

where

$$\alpha_{Fe}=\ln \gamma_{Fe}/(1-X_{Fe})^2 \qquad (49)$$

Therefore

$$\ln \gamma_{Fe}=[(15.06-30.07(\tfrac{1}{2}+X_{Fe})](1-X_{Fe})^2 \qquad (50)$$

From equation (50) the limiting activity coefficient of iron in liquid sulphur was estimated as $\gamma^{\circ}_{Fe(S)}=1.028$.

By the same method, taking $X_{PbS}=0.0001$ and $X_{PbS}=0.998$ from Fe-Pb binary (Fig.5) α function was expressed as

$$\alpha_{Fe}=5.5 \quad .37(\tfrac{1}{2}+X_{Fe}) \qquad (51)$$

And

$$\ln \gamma_{Fe}=[5.55+1.37(\tfrac{1}{2}+X_{Fe})](1-X_{Fe})^2 \qquad (52)$$

from equation (52) the limiting activity coefficient of iron in liquid lead was found as $\gamma^{\circ}_{Fe(Pb)}=510.71$.

Henrian activity coefficient and self interaction coefficient of sulphur at infinite dilution in liquid lead were calculated by using activity data of Eric[7] in Pb-PbS system as $\ln \gamma^{\circ}_{S(Pb)}=-4.49$ and $\varepsilon^{S}_{S}=-0.42$ after a relevant regression analysis in the interval of $0<X_S<0.16$, as shown in Figure 19. Although at first sight, $\ln \gamma_S$ versus X_S does not look absolutely linear, within this very narrow composition range, regression analysis gave a very high correlation coefficient of r=0.96, indicating that linear relationship is justified.

All the above mentioned thermodynamic information for the binaries was used in connection with the experimentally determined tie-line data (Table 2, Figure 16) to calculate a consistent set of activities along the miscibility gap of the Fe-Pb-S system at 1473K. Equation (42) permitted the calculation of the ratio $\ln(a_S/a_{Pb})$ along the lower lead rich boundary from which activities of iron, lead and sulphur were evaluated by the following integrated form of equations (39) and (40).

$$(\ln a_{Fe})_{(y_i)} = (\ln a_{Fe})_{(y_i=0)} + \int_0^{y_i} \Omega \, d\left(\ln \frac{a_S}{a_{Pb}}\right)_{(y_i)} \qquad (53a)$$

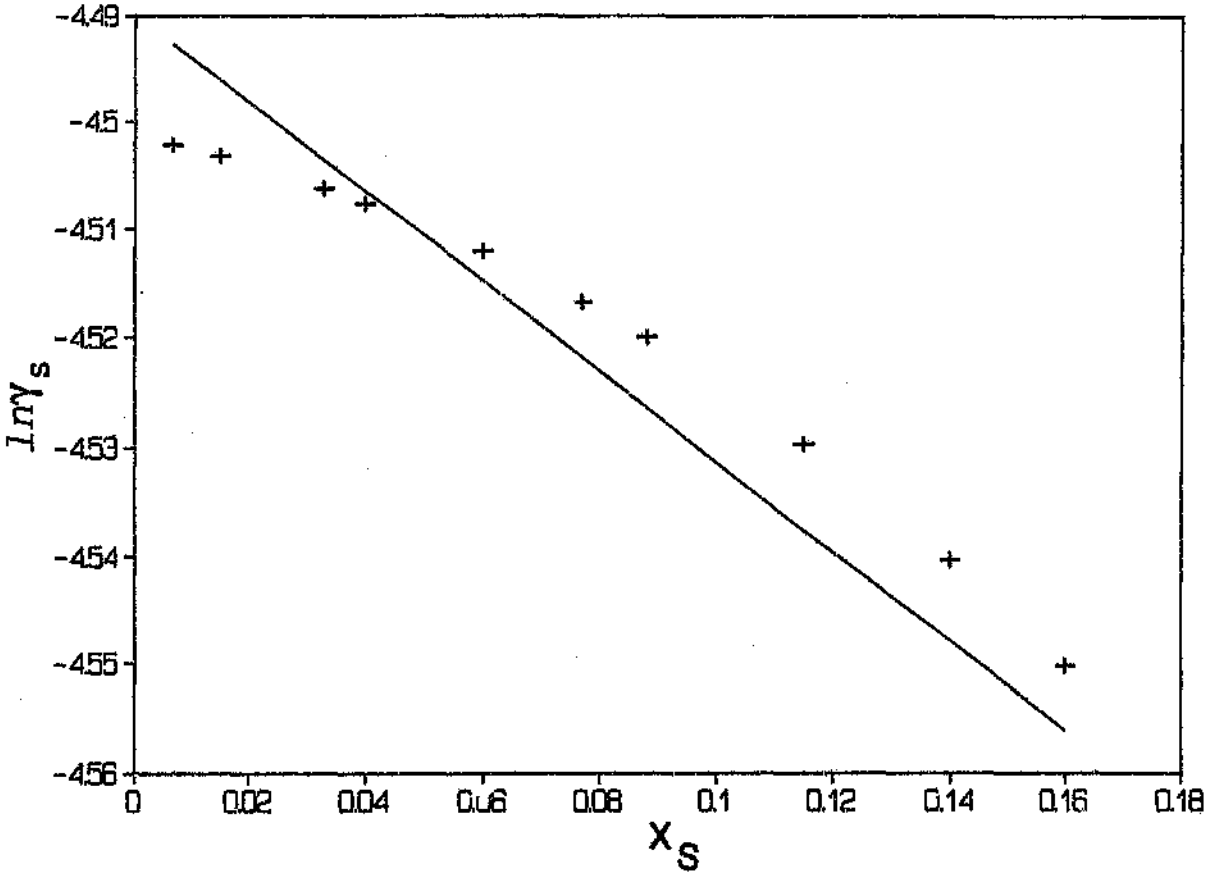


Figure 19. Activity coefficient of Sulphur versus mole fraction of Sulphur in Pb-S system.

$$(ln a_{Pb})_{(y_i')} = (ln a_{Pb})_{(y_i'=0)} + \int_0^{y_i'} \lambda \; d(\ln \frac{a_S}{a_{Pb}})_{(y_i')} \qquad (53b)$$

$$(ln a_S)_{(y_i')} = (ln a_S)_{(y_i'=0)} + \int_0^{y_i'} \theta \; d(\ln \frac{a_S}{a_{Pb}})_{(y_i')} \qquad (53c)$$

Where Ω, λ and θ are defined by:

$$\Omega = (y_S^* - y_S') / (y_{Fe}' - y_{Fe}^*) \qquad (54a)$$

$$\lambda = (y_S' \cdot y_{Fe}^* - y_S^* \cdot y_{Fe}') / (y_{Fe}' - y_{Fe}^*) \qquad (54b)$$

$$\theta = (y_{Pb}^* \cdot y_{Fe}' - y_{Pb}' \cdot y_{Fe}^*) / (y_{Fe}' - y_{Fe}^*) \qquad (54c)$$

The integrals of equations (53) were evaluated graphically as the area under the curves Ω, λ and θ against $\ln(a_S/a_{Pb})_{(ys)}$. These integration plots are shown respectively in Figures 21 of the Appendix.

All the thermodynamic data gathered with the precedure explained above, along the ternary miscibility gap of the Fe-Pb-S systems were used to construct the diagrams shown in Figures 20a, b and c, which show iso-activities of iron, lead and sulphur.

Since the tie-line distribution is known down to y^*_S=0.005 (tie line 1) from the experimental work, the uncertainties in the lower integration limits obtained by extrapolation of the activity values of lead and sulphur from the Pb-PbS binary are minimized.

The value of a_{Pb} and a_S at y^*_S =0.005 (tie-line 1) were taken as 0.993 and 5.6×10^{-5} respectively by utilizing the available activity coefficients and self interaction parameters stated above.

Activities of iron were calculated by taking the activity of Fe a_{Fe}=1 as reference on the bottom line of the miscibility gap drawn from Fe-FeS side towards the Pb corner separating two liquid region from the three phase region: $Fe(\gamma)+L_1+L_2$.

The calculated Fe, Pb and S activities on each tie-line through the method of Choudary and Chang[26,27] as outlined above are given in Table 4.

The uncertainty in the derived activities can be readily assessed by analyzing the individual uncertainties in various terms of equations (53). These equations are thermodynamically exact and the errors in the activities along the miscibility gap can be attributed to the uncertainties in a) the integration function Ω , λ and θ b) the calculation of activity ratio, and c) the integration procedure.

From the tie-line data presented in Table 2 and Figure 16 the maximum error in the integration function Ω , λ and θ due to the error of chemical

analysis is estimated to be ±0.015, ±0.02 and ±0.03. Referring to equation (42), the uncertainty in the calculated $\ln(a_S/a_{Pb})_{(y_S)}$ values along the miscibility gap are due to a) the errors in the binary Pb-S activity data and b) the errors in the term of the right hand side of equation (42) which consists of y^*_{Fe} and the term in the bracket. The term in the bracket was derived from the quasichemical model of Jacob and Jeffes[30]. The derived values are reported by Choudary et al[26] to have an uncertainty of ±20%.

Even if 40% uncertainty is assumed for the values of this term, with that of ±0.05 in the values of $\ln(a_S/a_{Pb})$ in the Pb-S binary and of ±0.03 in Y^*_{Fe}, the derived values of $\ln(a_S/a_{Pb})$ along the miscibility gap will not be in error by more than ±0.22 units.

The last source of error is due to the graphical integration procedure. It can well be seen that the integration functions Ω, λ and θ result in very smooth curves in which integration errors would be negligible. Therefore, the total uncertainty in activity values is not expected to be greater than 10%.

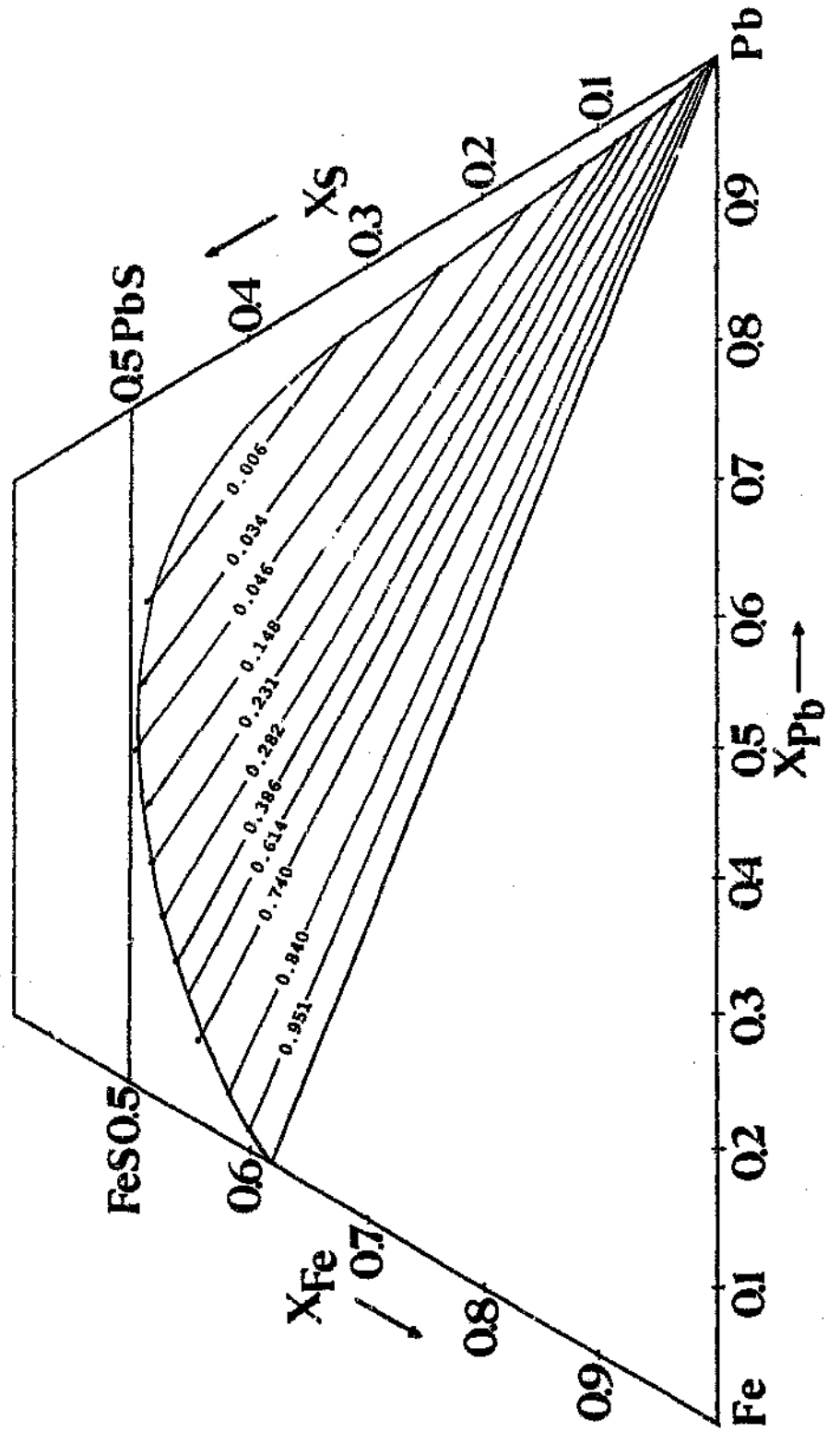


Figure 20a. Iso-activities of Fe in Fe-Pb-S melts at 1200°C

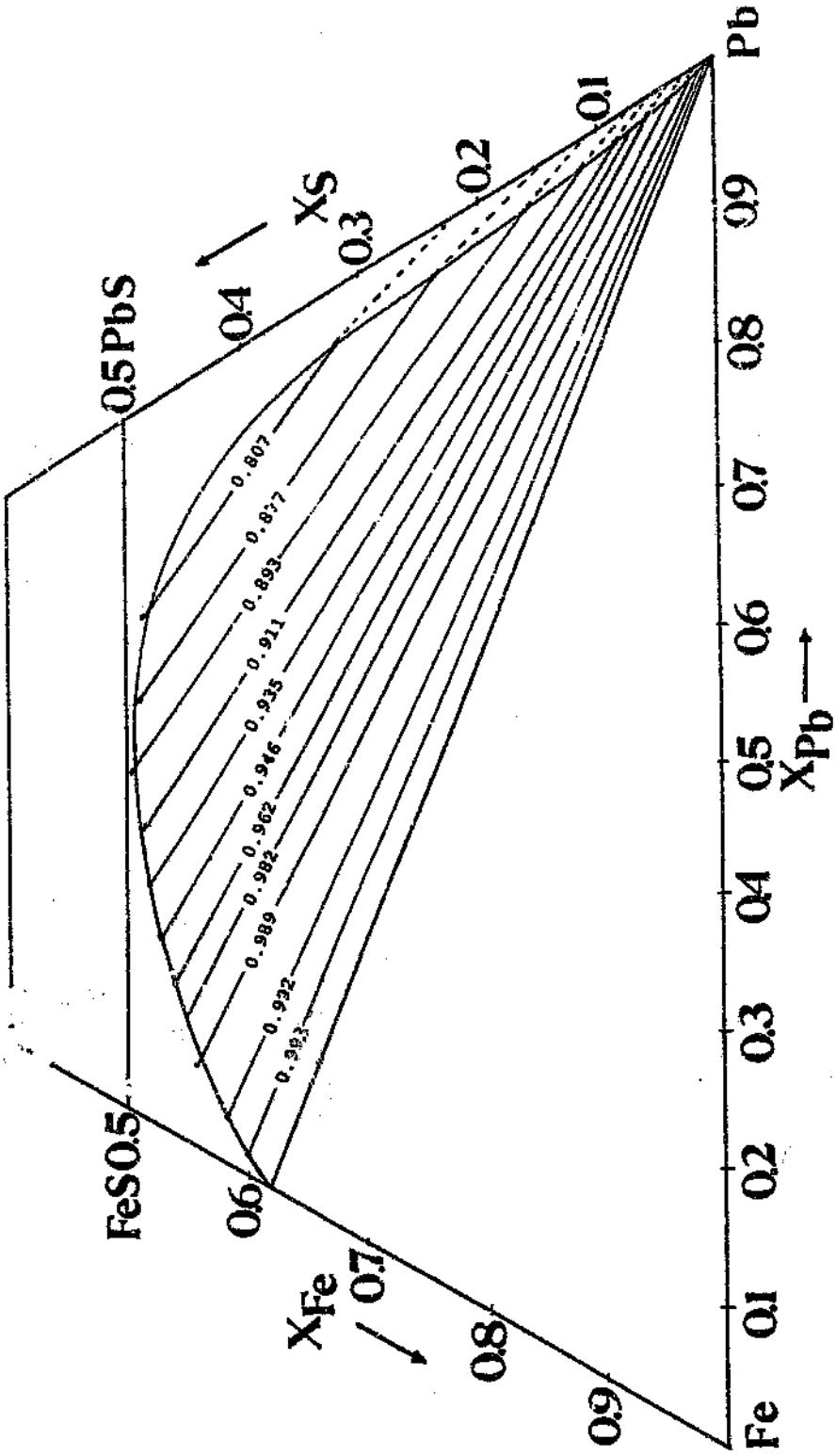


Figure 20b. Iso-activities of lead in Fe-Pb-S melts at 1200°C.

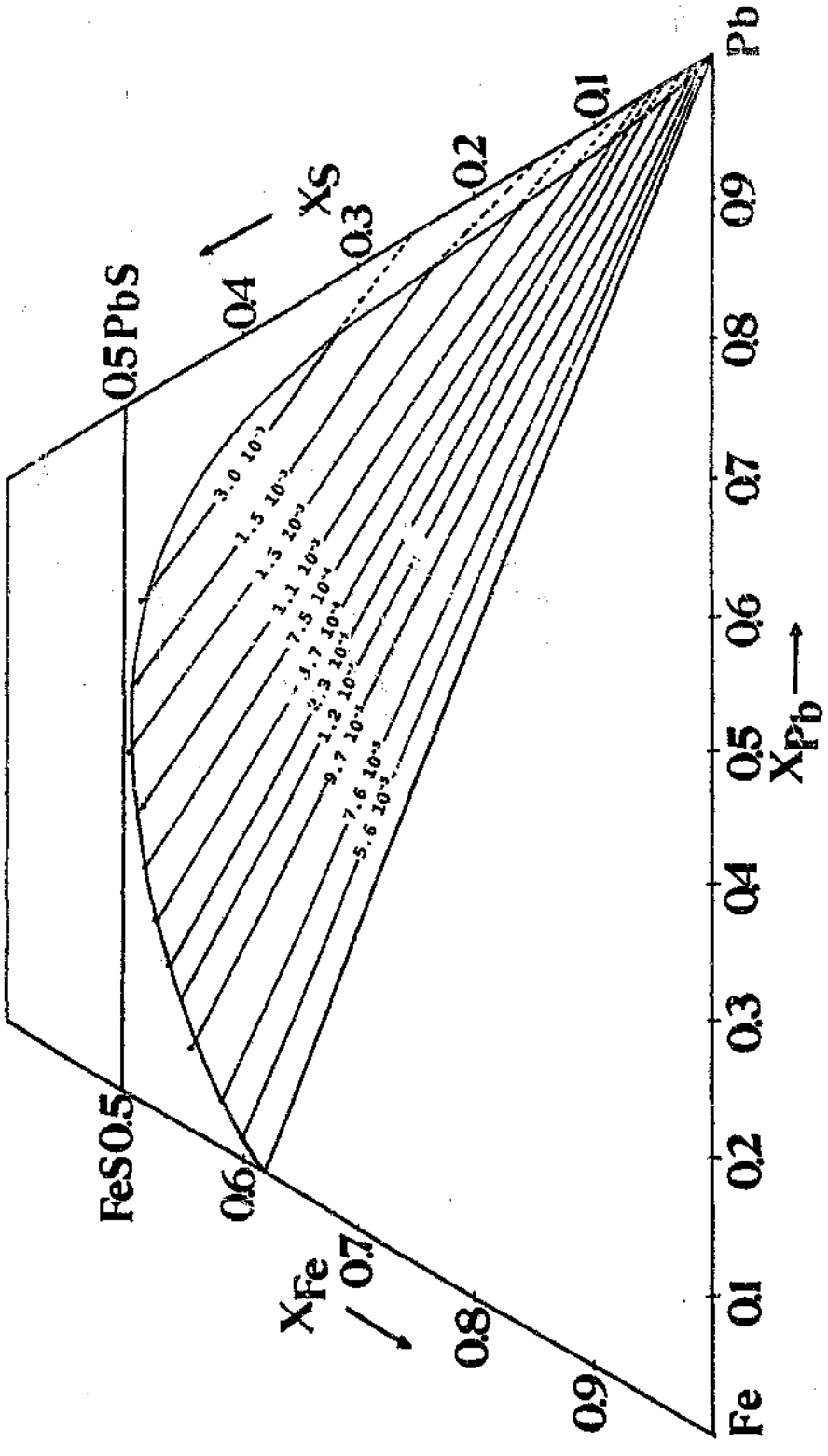


Figure 20c. Iso-activities of S in Fe-Pb-S melts at 1200°C.

ii) Activity calculations by Gibbs-Duhem ternary integration:

The activities of Pb at 1200°C along the sulphur saturation boundary of the ternary miscibility gap were determined by measurement of the dew-point temperatures of samples selected from the lead-rich ends of the previously determined tie-lines. Pb activities were determined by the same method as described in section 4.2.1. by inserting dew-point temperatures into equation 12. Measured lead activities are also given in Table 4.

Since the sulphide saturated end of the tie-line (no 9) was very close to the FeS-PbS binary on which activity data at 1200°C is available in this study, it was decided to use ternary Gibbs-Duhem equations to calculate activities of Fe and S by using experimentally measured activities of Pb.

For the sulphide-saturated liquid phase:

$$X_{Fe}\,d\log a_{Fe}+X_{Pb}\,d\log a_{Pb}+X_{s}\,d\log a_{s}=0 \qquad (55)$$

For the lead-rich liquid phase:

$$X'_{Fe}\,d\log a_{Fe}+X'_{Pb}\,d\log a_{Pb}+X'_{s}\,d\log a_{s}=0 \qquad (56)$$

When equation (55) is multiplied by X'_S and equation (56) by X_S, and the terms with $d\log a_S$ are eliminated, the following equation is obtained for the activity of iron:

$$d\log a_{Fe}=\Phi\, d\log a_{Pb} \qquad (57)$$

where the composition parameter Φ was given by

$$\Phi = -(X'_S X_{Pb} - X_S X'_{Pb}) / (X'_S X_{Fe} - X_S X'_{Fe}) \quad (58)$$

The integral of equation 57 can be written as

$$\log a_{Fe} = \log a^*_{Fe} + \int_{a^*_{Pb}}^{a_{Pb}} \Phi \, d\log a_{Pb} \quad (59)$$

This integral can be performed to evaluate $\log a_{Fe}$ when $\log a^*_{Fe}$ at the starting point of integration is known, and when the data on a_{Pb} are sufficiently complete as a function of parameter Φ. The tie-line number 9 on which $a_{Pb}=0.894$ served as starting line. At that point, the sulphide activities were taken as $a_{PbS}=0.411$ and $a_{FeS}=0.384$ from the activity data available in this study for FeS-PbS binary solutions (Table 3a).

By use of the measured a_{Pb} and a_{PbS} from this study and the standard free energy of liquid PbS[14] at 1200°C (equation 11), the partial pressure of sulphur on this tie-line was found to be 3.8×10^{-4} atm. From the standard free energy of formation of liquid FeS (equation 15), the available $a_{FeS}=0.384$ value, and P_{S2} as calculated above, a_{Fe} on this particular tie-line was calculated as $a^*_{Fe}=0.045$. With this value as the starting point, the integral of equation (59) was evaluated as the area under the curve for Φ against $\log a_{Pb}$.

The sulphur activity at starting point was found to be $a^*_S=1.3\times10^{-3}$ from the standard free energy change of reaction (13) by employing sulphur partial pressure of 3.8×10^{-4}atm on this particular line.

After elimination of $dloga_{Fe}$ terms from equations (55) and (56), the final equation for sulphur activity was found as

$$loga_S = loga_S^* + \int_{a_{Pb}^*}^{a_{Pb}} \Psi \, dloga_{Pb} \qquad (60)$$

where

$$\Psi = -(X'_{Fe}X_{Pb} - X_{Fe}X'_{Pb}) / (X'_{Fe}X_{S} - X_{Fe}X'_{S}) \qquad (61)$$

Again with the known value of $a_S^* = 1.3 \times 10^{-3}$ at the starting point, the integral of equation (60) was evaluated as the area under the curve for Ψ against $loga_{Pb}$.

The results of activity calculations by ternary Gibbs-Duhem integration are given in Table 4 together with the results obtained from the method of Choudary and Chang[26, 27] for comparison. As can be seen the agreement is excellent also providing the fact that the experimental methods involved in both phase equilibria and activity determinations are sound.

It should be mentioned that the iron and sulphur activities calculated by the help of Φ and Ψ functions of equations 59 and 60 are sensitive to the slopes of these functions. Plots were drawn for Φ and Ψ with respect to the logarithm of activity of lead after successive iterations so that for example the known activity of iron ($a_{Fe}=1.0$) along the straight line from the Fe-FeS side to Pb corner could be obtained within 0.002 units.

This procedure yielded a set of activities consistent with the phase relations, and the excellent agreement of activities obtained by two different methods strongly support this.

	Activities Calculated by the Method of Choudary et al[26,27]			Activities Calculated by Ternary Gibbs-Duhem Integration			
Tie-Line Number	a_{Fe}	a_{Pb}	a_S	Dew-Point Temperatures (°C)	a_{Pb} (measured)	a_{Fe}	a_S
1	0.951	0.993	$5.6\ 10^{-5}$	-	-	-	-
2	0.840	0.992	$7.6\ 10^{-5}$	1199.4	0.994	0.842	$7.4\ 10^{-5}$
3	0.740	0.989	$9.7\ 10^{-5}$	-	-	-	-
4	0.614	0.982	$1.2\ 10^{-4}$	1198.5	0.984	0.624	$1.3\ 10^{-4}$
5	0.386	0.962	$2.3\ 10^{-4}$	-	-	-	-
6	0.282	0.946	$3.7\ 10^{-4}$	1194.3	0.948	0.285	$3.9\ 10^{-4}$
7	0.231	0.935	$7.5\ 10^{-4}$	-	-	-	-
8	0.148	0.911	$1.1\ 10^{-3}$	1191.0	0.910	0.146	$1.1\ 10^{-3}$
9	0.046	0.893	$1.3\ 10^{-3}$	1189.1	0.894	0.045	$1.3\ 10^{-3}$
10	0.034	0.877	$1.5\ 10^{-3}$	-	-	-	-
11	0.006	0.807	$3.0\ 10^{-3}$	1177.5	0.796	0.006	$3.2\ 10^{-3}$

Table 4. The results of activity calculations in the system Fe-Pb-S at 1473K.

SUMMARY AND CONCLUSIONS

The aim of this investigation was to generate thermodynamic and phase relations data on lead containing sulphide systems by using the dew-point and quenching technique of thermochemical research. The specific systems selected for thermodynamic consideration during this study were:

1.) FeS-PbS binary system
2.) The Fe-Pb-S ternary system

The information gathered with respect to the above systems were the following:

1.) High temperature phase relations in the FeS-PbS system were examined by quenching technique. Eutectic temperature of this system was found at 46 atomic percent PbS at 842°C. Activity measurements were carried out in this system at 1200 and 1100°C by measuring dew-point temperatures of PbS. Activities showed negative deviations from ideality. The FeS-PbS liquid solutions were modelled and PbS and FeS activities were calculated by applying the Krupkowski formalism. Liquidus lines, eutectic temperature and composition of the FeS-PbS phase diagram calculated through formalism were in complete agreement with results obtained experimentally.

2.) In Fe-Pb-S melts, the immiscibility region and the direction of conjugation lines between liquid matte and liquid metal phases at 1200°C were found by quenching experiments. The activities of lead along the ternary miscibility gap were measured by the dew-point technique at 1200°C. Using the measured lead activities, activities of iron and sulphur were calculated through ternary Gibbs-Duhem integration.

In addition, the activities of lead, iron and sulphur along the ternary miscibility gap of the Fe-Pb-S system were calculated through the recent method developed by Choundary and Chang[26,27], from the tie-line distributions and thermodynamic information of the bounding binaries Pb-PbS, Fe-FeS and Fe-Pb. Both of the results obtained from these two methods were in good agreement. The distribution of tie-lines were in accordance with the behaviour of activity in both Pb-PbS and FeS-PbS melts.

The sulfide melts studied in this study are not simple stoichiometric mixtures of FeS and PbS but may contain additional species like Fe, Pb and S as the result of dissociation reactions common to these compounds in liquid state. An estimate on FeS dissociation can be obtained from the thermodynamic analysis presented by Sharma and Chang[9] for Fe-S liquid solutions; their approach yields that at 1200°C the ferrous sulfide liquid phase will contain X_{FeS}=0.9770, X_{Fe}=0.00115, and X_S=0.0115. For the same reasons as described for Fe-S melts[9], the Pb-S melts can be regarded to consist of the species PbS, Pb and S. The concentrations of these species are governed by the equilibrium:

$$PbS(l)=Pb(l)+S(l) \qquad (62)$$

for which the following equilibrium constant expression can be developed from the data available in literature[39,40,41].

$$\ln K= -5652/T - 13.784 + 1.630 \ln T \qquad (63)$$

In the Pb-S phase diagram, the lead rich solidus of

PbS has X_{Pb}=0.50021 and X_S=0.49979 near the melting point of PbS[42]. Using these and the value of K at 1200°C from equation (63) the dissociation of PbS can be treated in a manner similar to the method described by Lumsden[43], this procedure reveals that the composition of the molten lead sulfide at 1200°C is X_{PbS}=0.983, X_{Pb}=0.009 and X_S=0.008.

It appears from the preceding discussion that FeS and PbS do not dissociate extensively at 1200°C. Therefore, although the sulfide melts are not strictly stoichiometric, their compositions can be represented adequately in terms of the end-member compounds. This conclusion is also supported by the results of occasional chemical analyses done on sulphide samples.

REFERENCES

1. Friedrich, K. The solidification in the Pseudobinary Systems: PbS-FeS and PbS-AgS_2, Metallurgie, 1907, 4(14),479-485.

2. Kopylov, N. I., and Novoselov, S.S., The FeS-PbS system, Metallurgicheskaye i Khim Promyshlennost, Kazakhstan, 1962, (1),53.

3. Kerby, R.C., Phase Equilibria and Matte Solidification in the Ternary System ZnS-FeS-PbS, Canad. Mines Bur. Invest., Rep. No. IR 73-49, 1973, Dept. of Energy, Mines and Resources, Ottawa, pp. 118

4. Brett, P. R. and Kullerud, G., The Fe-Pb-S System, Econ, Geol., 1967, 6213, 354-369.

5. Kullerud, G., The lead-Sulphur System, Carnegie Inst. Washington Year Book, 1965, vol.64 pp. 195-197.

6. Kullerud, G., The lead-sulphur system, Am. J. of Science, 1969, vol. 267-A, pp.233-256.

7. Eriç, R. H. and Timuçin, M., Phase equilibria and thermodynamics in the Lead-Lead Sulphide System, J. of SA.I.M.M., Nov.1988, pp 353-361.

8. Hillert, M. and Staffanssons, L. I., A Thermodynamic Analysis of the Phase Equilibria in the Fe-Mn-S System, Metal Trans. B, 1976 vol. 7B, pp 203-11.

9. Sharma, R. C. and Chang, Y. A., Thermodynamic and Phase Relationships of Transition Metal-Sulfur Systems, Thermodynamic Properties of the FeS Liquid Phase and the calculation of the Fe-S phase diagram, **Metal Trans**, 1976., vol.10B, pp 103-108.

10. Fernandez, A., Guillermet, M, Hillert, M. Jannson, B. Sundman, B., An Assessment of the Fe-S System using a Two-Sublattice Model for the Liquid Phase, **Metall. Trans.B**, 1981, vol.12B, pp 745 - 54.

11. Chuang, Y. Y., Hsieh, K. and Austin Cheng, Y., Thermodynamic and Phase Relationship of Transition Metal Sulphide Systems. A reevaluation of the Fe-S system using an Associated solution Model for the Liquid Phase, **Metal Trans.** B, 1985, pp 277 - 285.

12. Kubaschewski, O., Iron-Lead, **Iron-Binary Phase Diagrams**, Springer-Verlag, Berlin, 1982, pp 125 - 128 .

13. Brett, P. R. and Kullerud, G., The Fe-Pb-S System, **Carnegie Inst. Washington, Yearbook**, 1964, 63, pp 202 - 204 .

14. Schuhmann, R., Pei-Chen Chen, Jr., Palanisamy, P. and Sarma, D. H., **Metal. Trans.** B, 1976, vol. 78, pp. 95 - 101.

15. Elliot, J.F., and Gleiser, M., **Thermochemistry for steelmaking**, 1960, vol. 1, Reading (Massachusetts), Addison - Wesley.

16. Shamsuddin, A., Thermodynamic studies ... lead sulphide, **Met. Trans.** B., 1977, vol 8B, pp 349 - 352.

17. Davey and Joffre: Vapour Pressures and Activities of SnS in Tin-Iron mattes, **Trans. J.M.M.**, 1973, Vol. C82. pp 145 - 50.

18. Eriç, H. and Timuçin, M., Activities in Cu_2S - FeS - PbS melts at 1200°C, **Metal. Trans**, B, 1981, Vol.12 B, pp. 493 - 500.

19. Nesterov, V. N., Isakova, R. A. and Shendyapin, A. S., **Russ. J. Phys. Chem**, 1969, vol. 43 pp. 1785 - 88.

20. Hansen, M. and Anderko, K., **Constitution of Binary Alloys**, 2nd ed. McGrawn - Hill Book Company, New York, 1973.

21. Rosenqvist, T., Thermodynamic Study of Iron, Cobalt and Nickel Sulphides, **J. Iron Steel Inst**, 1954, vol.176,p.37-57.

22. Bale, C. W. and Toguri. J. M., Technique to measure the Thermochemical Properties of Liquid Metal-Oxygen-Sulphur Systems and Its Application to Restricted Regions of the Iron-Sulphur-Oxygen and Copper-Sulphur-Oxygen Systems at 1200°C, **Can.Met.Quart**,1976, Vol. 15, p. 305.

23. Colin, R. and Drowat, J., Thermodynamic study of tin sulphide and lead sulphide using a mass spectrometer, **J. of Chem.Phys**, vol 37.1962. pp. 1120 - 1125.

24. Eriç, R. H., Ph.D. Thesis, Middle East Technical University, Ankara, 1979.

25. Birchenall, C. E. and Cheng, C. H., The vapour Pressure of Zinc and Cadmium over some of their Silver Alloys, **Metal. Trans**, (JOM), 1949, vol.185, pp 426-434.

26. Choundary, U. V. and Chang, Y. A., A Thermodynamic Method for Determining the Activities from Ternary Miscibility Gap Data. The Copper-Lead-Oxygen System, **Metall.Trans**, B, 1976, Vol.7B, pp 655-60.

27. Choundary, U. V., Lee, Y. E. and Chang, Y. A., A Thermodynamic Analyses of the Copper-Lead-Sulphur System at 1473 K, **Metall.Trans.** B, 1977, Vol.8B, pp 541-545.

28. Chipman, J., Thermodynamics of Binary and Ternary solutions containing one interstitial Solute, **Metall.Trans.**B, 1972, Vol.3, pp 879-885.

29. Wagner, C., Thermodynamics of Alloys, **Metall.Trans.** B, 1975, Vol.6B, pp 395-398.

30. Jacob, K. T. and Jeffes, J. H. E., Thermodynamics of Oxygen in Liquid Copper, and Copper-Lead Alloys, **Trans.Inst.Mining.Met.**, 1971, vol.C80, pp.32-41.

31. Wriedt, H. A., Calculation of Activities in Binary Systems having Miscibility Gaps. **Trans. TMS-AIME**, 1961, Vol.221, pp 377-383.

32. Hardy, H. K., A Sub-Regular Solution Model and its Application to some Binary Alloy Systems, **Acta Met.**, 1953, vol.1, pp. 202-209.

33. Krupkowski, A., **Bull.Acad.Polon.Sci.Lett.**, Ser.A., 1950,vol.1.pp. 15-45.

34. Moser, Z., Thermodynamic Behaviour in Binary Metallic Solutions, Metal. Trans., B, 1975, vol.6, pp. 653 - 659.

35. Kellog, H. H., Vaporization chemistry in extractive metallurgy, Trans. TMS-AIME, vol. 236, pp. 602-615.

36. Brett, P. R. and Kullerud, G., The Fe-Pb-S system, Carnegie Inst. Washington, Yearbook, 1962, 61, pp. 196 - 197.

37. Yazawa, A., Gubcova, A. and Ujiie, H., Bull. Res, Inst. Miner. Dressing Metallurgy, Sendai. Tohuku Univ., 1968, vol. 24 p. 105-106.

38. Davey, T. R. and Willis, G. M., J. Met., March 1977, vol. 29, p. 24-30.

39. Shamsuddin, Metall. Trans., B, 1977, vol 8B, pp. 349-52.

40. Stubbles, J. R. and Birchenall, C. E., Trans. TMS-AIME, 1959, vol. 215, p. 535-38.

41. JANAF Thermochemical Tables, 2nd ed. U.S. Dept. of commerce (Nat. Bur. Stand.), 1971.

42. Bloem, J. and Kröger, F. A., J. Phys. Chem., 1956, vol. 7, p. 1-14.

43. Lumsden, J., Thermodynamics of Molten Salt Mixtures, Academic Press, London and New York, 1966, p. 312-13.

7. APPENDIX

Integration Functions of Fe, Pb and S in Fe-Pb-S system. The Ω , λ and θ functions which were used in the method developed by Choudary and Chang[26,27] to derive Fe,Pb and S activities along the ternary miscibility gap of the system Fe-Pb-S at 1200°C are illustrated in Figures A.21a, A.21b and A.21c respectively. The Φ and Ψ functions employed in the calculation of iron and sulphur activities by the classical ternary Gibbs-Duhem integration as shown in Figures A.22a and A.22b.

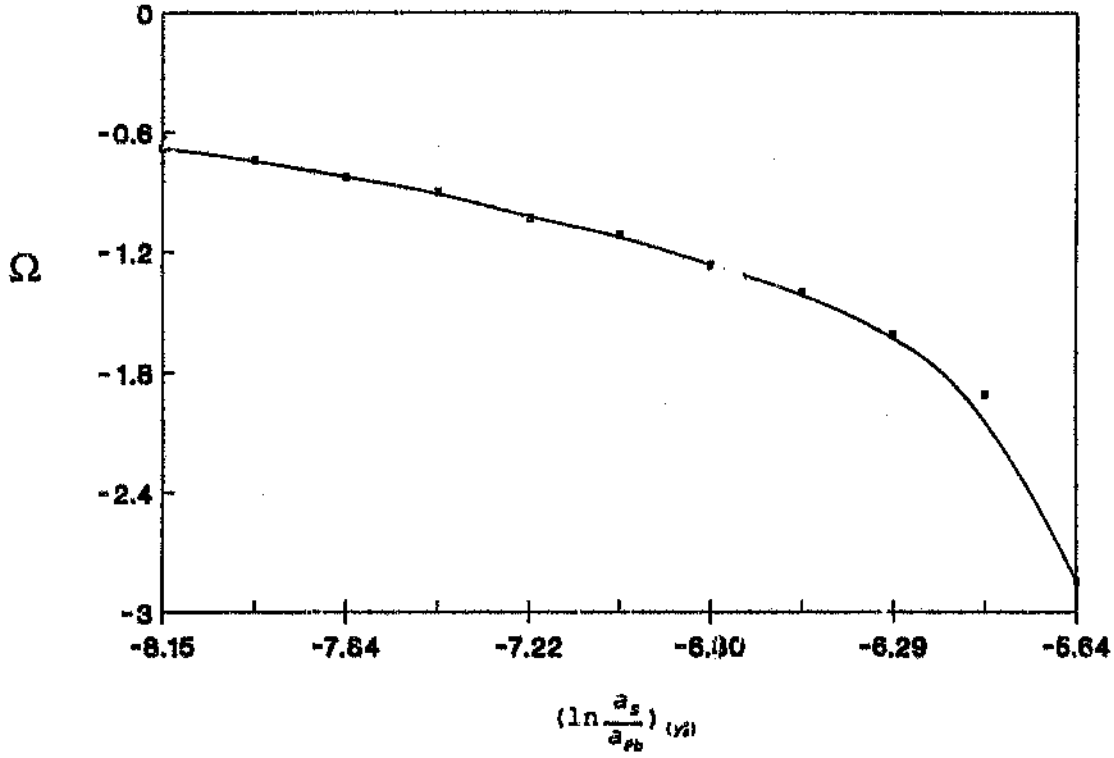


Figure A.21a. The Integration function Ω against $\ln(a_S/a_{Pb})$ used to evaluate Fe activities in the system Fe-Pb-S at 1200°C

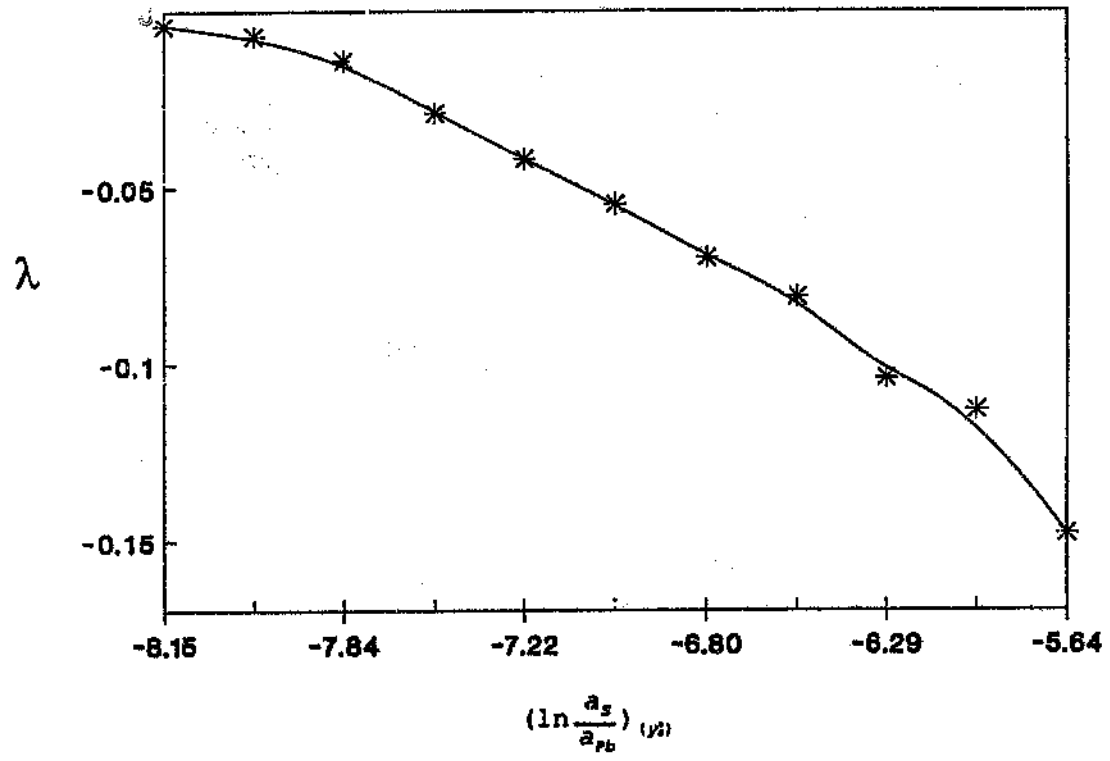


Figure A.21b. The integration function λ against $\ln(a_S/a_{Pb})$ used to evaluate Pb activities in the system Fe-Pb-S at 1200°C.

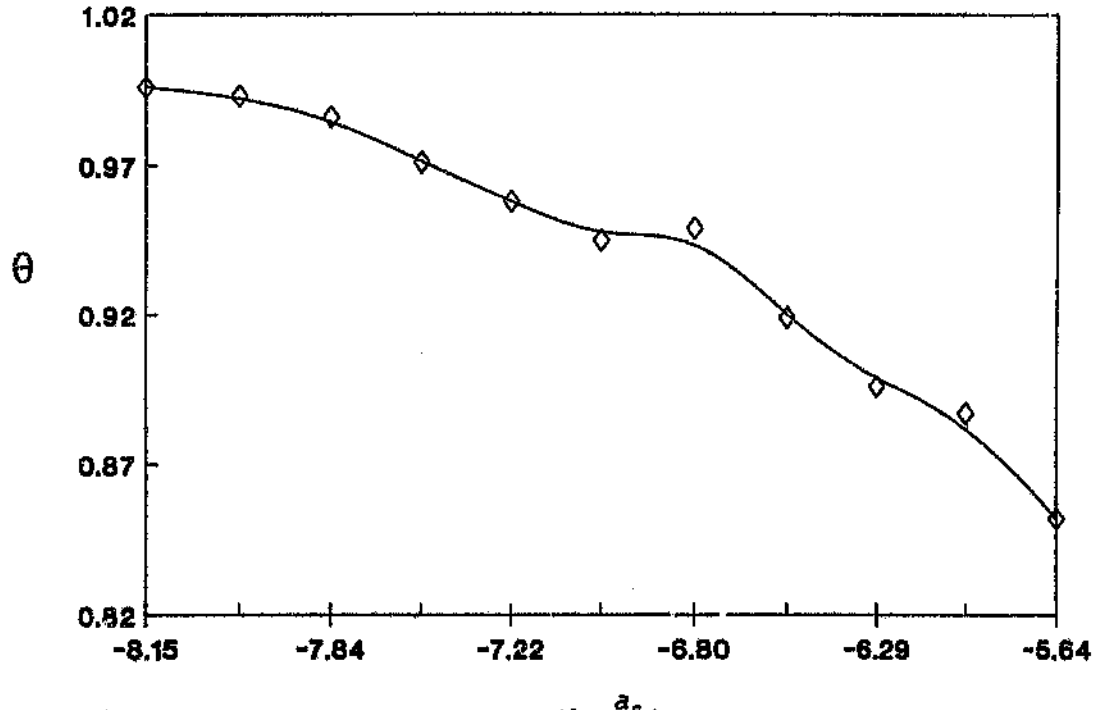


Figure A.21c. The integration function θ against $\ln(a_S/a_{Pb})$ used to evaluate S activities in the system Fe-Pb-S at 1200°C.

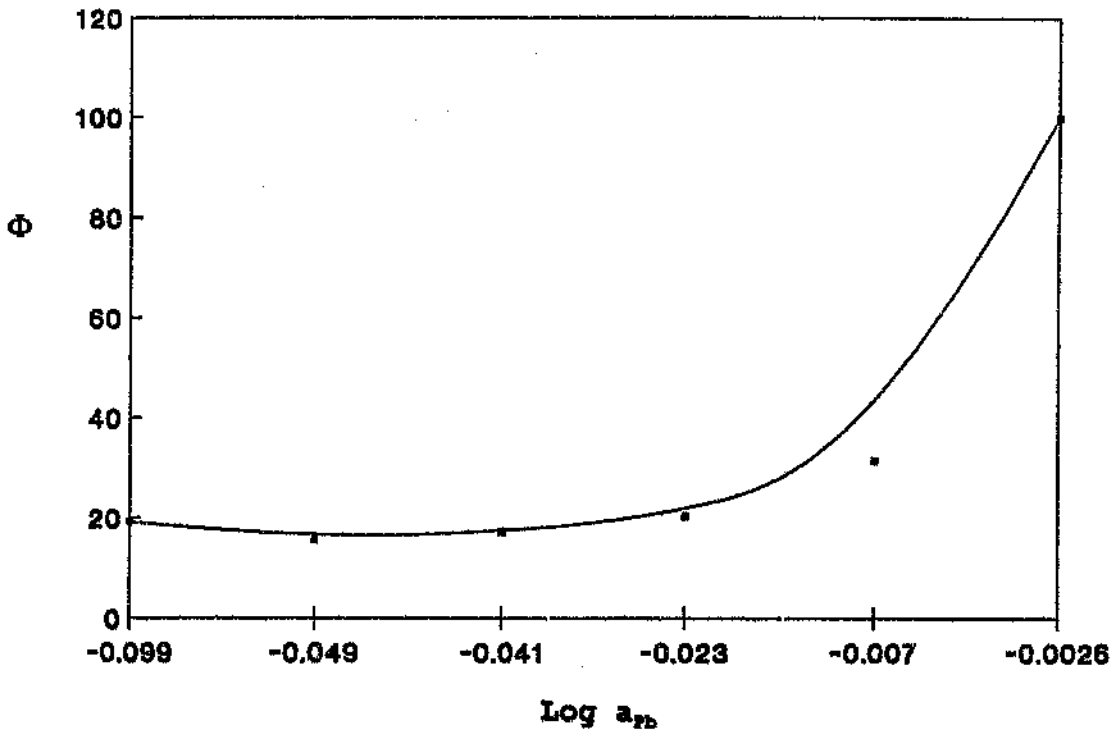


Figure A.22 a. The integration function Φ against $\log a_{Pb}$ used to evaluate Fe activities in the system Fe-Pb-S at 1200°C.

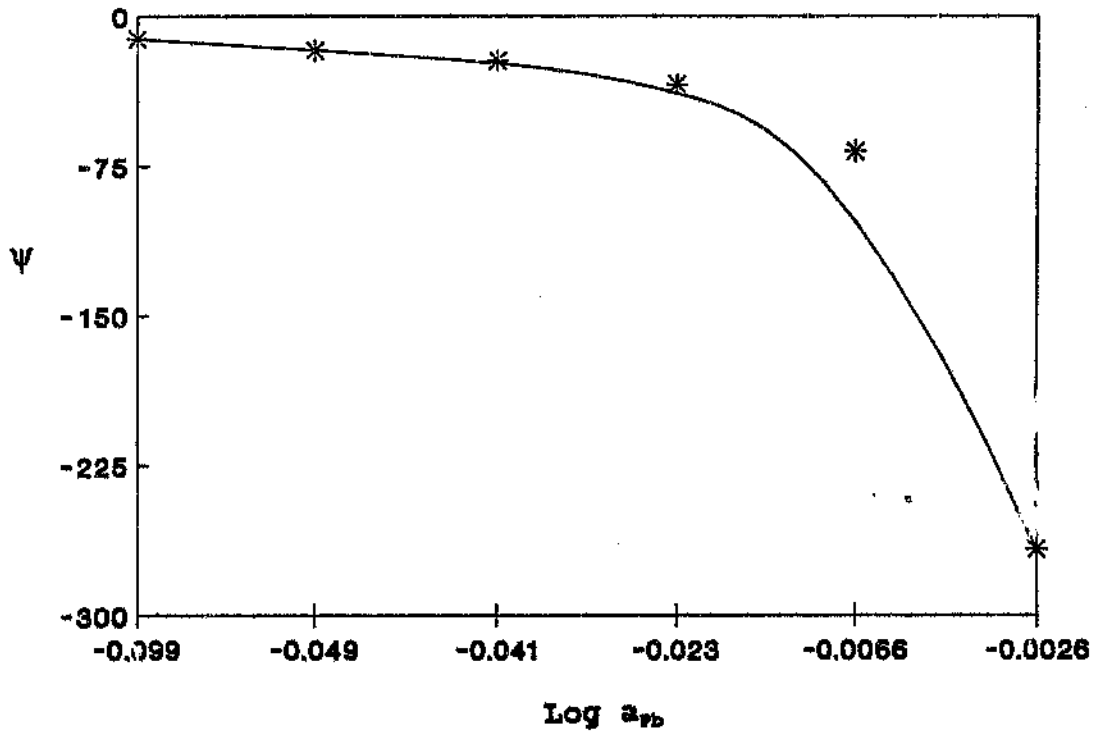


Figure A. 22 b. The integration function Ψ against $\log a_{Pb}$ used to evaluate S activities in the system Fe-Pb-S at 1200°C.

Author: Ozok Hakan.
Name of thesis: Phase relation and thermodynamics in Iron-lead-sulphur system.

PUBLISHER:
University of the Witwatersrand, Johannesburg
©2015

LEGALNOTICES:

Copyright Notice: All materials on the University of the Witwatersrand, Johannesburg Library website are protected by South African copyright law and may not be distributed, transmitted, displayed or otherwise published in any format, without the prior written permission of the copyright owner.

Disclaimer and Terms of Use: Provided that you maintain all copyright and other notices contained therein, you may download material (one machine readable copy and one print copy per page)for your personal and/or educational non-commercial use only.

The University of the Witwatersrand, Johannesburg, is not responsible for any errors or omissions and excludes any and all liability for any errors in or omissions from the information on the Library website.